

EFFECT OF ERIANTHRIDIN ON NON-SMALL CELL LUNG CANCER CELL METASTASIS



A Thesis Submitted in Partial Fulfillment of the Requirements
for the Degree of Master of Science in Pharmacy in Pharmacology and Toxicology
Department of Pharmacology and Physiology
FACULTY OF PHARMACEUTICAL SCIENCES
Chulalongkorn University
Academic Year 2020
Copyright of Chulalongkorn University

ผลของอิริแอนทรินต่อการแพร่กระจายของเซลล์มะเร็งปอดชนิดไม่ใช่เซลล์เล็ก



วิทยานิพนธ์นี้เป็นส่วนหนึ่งของการศึกษาตามหลักสูตรปริญญาเภสัชศาสตรมหาบัณฑิต

สาขาวิชาเภสัชวิทยาและพิษวิทยา ภาควิชาเภสัชวิทยาและสรีรวิทยา

คณะเภสัชศาสตร์ จุฬาลงกรณ์มหาวิทยาลัย

ปีการศึกษา 2563

ลิขสิทธิ์ของจุฬาลงกรณ์มหาวิทยาลัย

Thesis Title	EFFECT OF ERIANTHRIDIN ON NON-SMALL CELL LUNG CANCER CELL METASTASIS
By	Miss Sutthaorn Pothongsrisit
Field of Study	Pharmacology and Toxicology
Thesis Advisor	Associate Professor VARISA PONGRAKHANANON, Ph.D.

Accepted by the FACULTY OF PHARMACEUTICAL SCIENCES, Chulalongkorn University in Partial Fulfillment of the Requirement for the Master of Science in Pharmacy

..... Dean of the FACULTY OF
PHARMACEUTICAL SCIENCES
(Assistant Professor RUNGPETCH SAKULBUMRUNGSI,
Ph.D.)

THESIS COMMITTEE

..... Chairman
(Associate Professor SUREE JIANMONGKOL, Ph.D.)

..... Thesis Advisor
(Associate Professor VARISA PONGRAKHANANON, Ph.D.)

..... Examiner
(VISARUT BURANASUDJA, Ph.D.)

..... External Examiner
(KRIENGSAK LIRDPRAPAMONGKOL, Ph.D.)

สุทธอร โพธิ์ทองศรีสิทธิ์ : ผลของอีริแอนทรีดินต่อการแพร่กระจายของเซลล์มะเร็งปอดชนิด
 ไม่ใช่เซลล์เล็ก. (EFFECT OF ERIANTHRIDIN ON NON-SMALL CELL LUNG CANCER
 CELL METASTASIS) อ.ที่ปรึกษาหลัก : รศ. ภญ. ดร.วริษา พงศ์เรขานานนท์

มะเร็งปอดเป็นมะเร็งที่มีอัตราการเสียชีวิตของผู้ป่วยเป็นอันดับต้น ๆ เนื่องจากการ
 แพร่กระจายของเซลล์มะเร็ง การแพร่กระจายของเซลล์มะเร็งประกอบด้วยหลายขั้นตอนโดยเริ่มจาก
 เซลล์มะเร็งเคลื่อนย้ายออกจากก้อนมะเร็งปฐมภูมิเข้าสู่ระบบไหลเวียนโลหิตไปยังส่วนอื่น ๆ ของร่างกาย
 และเกิดการเจริญเติบโตเป็นมะเร็งทุติยภูมิ การเคลื่อนที่และการบุกรุกของเซลล์มะเร็งเป็นขั้นตอนต้น ๆ
 ที่สำคัญของการแพร่กระจายของเซลล์มะเร็ง โดยเกี่ยวข้องกับการปรับเปลี่ยนโครงสร้างของแอกทินและ
 การปล่อยเอนไซม์เมทริกซ์เมทัลโลโปรตีนเอสเพื่อย่อยสลายสารระหว่างเซลล์ ซึ่งการยับยั้งกระบวนการ
 ดังกล่าวสามารถยับยั้งการแพร่กระจายของเซลล์มะเร็งได้ สารอีริแอนทรีดินเป็นสารประกอบฟีนอลิกที่
 พบได้ในกล้วยไม้ไทยสกุลหวายและมีฤทธิ์ทางเภสัชวิทยาหลายชนิด แต่ยังไม่มีการศึกษาฤทธิ์ทางเภสัช
 วิทยาที่เกี่ยวข้องกับการแพร่กระจายของเซลล์มะเร็งปอด จากผลการศึกษาพบว่าความเข้มข้นของสารอีริ
 แอนทรีดินที่ไม่เป็นพิษต่อเซลล์และไม่มีผลต่อการเจริญเติบโตของเซลล์สามารถลดการเคลื่อนที่และการ
 บุกรุกของเซลล์มะเร็งปอดได้ ผ่านทางการยับยั้งการจัดเรียงตัวของแอกทินและการเปลี่ยนแปลงรูปร่าง
 ของเซลล์เมมเบรนทำให้เซลล์มะเร็งปอดไม่สามารถสร้างขาเทียมที่ใช้สำหรับการเคลื่อนที่ได้ นอกจากนี้
 สารอีริแอนทรีดินสามารถลดการแสดงออกของเมทริกซ์เมทัลโลโปรตีนเอสชนิด 2 และ 9 ซึ่งเป็นเอนไซม์
 สำคัญที่เซลล์ใช้ในการย่อยสลายเนื้อเยื่อโดยรอบของเซลล์มะเร็ง การศึกษาเชิงกลไกแสดงให้เห็นว่าสารอีริ
 แอนทรีดินสามารถยับยั้งการทำงานของวิถีสัญญาณเอเคทีและเอ็มทอร์ซึ่งเป็นวิถีสัญญาณที่สำคัญในการ
 ควบคุมการเคลื่อนที่และการบุกรุกของเซลล์มะเร็ง โดยสารอีริแอนทรีดินสามารถเข้าไปจับกับโปรตีน
 เอเคทีได้โดยตรงจึงเป็นสาเหตุให้ยับยั้งการทำงานของโปรตีนดังกล่าวได้ จากการศึกษาดังกล่าวจึงแสดงให้เห็น
 เห็นว่าอีริแอนทรีดินเป็นสารที่น่าสนใจในการพัฒนาไปเป็นสารที่ใช้ต้านการแพร่กระจายของเซลล์มะเร็ง
 ปอดได้

สาขาวิชา เภสัชวิทยาและพิษวิทยา ลายมือชื่อนิสิต

ปีการศึกษา 2563 ลายมือชื่อ อ.ที่ปรึกษาหลัก

6270031533 : MAJOR PHARMACOLOGY AND TOXICOLOGY

KEYWORD: Erianthridin / Cell migration and invasion / Actin stress fibers /
Lamellipodia / Protein kinase B / Mammalian target of rapamycin

Sutthaorn Pothongsrisit : EFFECT OF ERIANTHRIDIN ON NON-SMALL CELL LUNG
CANCER CELL METASTASIS. Advisor: Assoc. Prof. VARISA PONGRAKHANANON,
Ph.D.

Lung cancer is one of leading cause of deaths worldwide due to cancer metastasis. The metastatic process that initiated by dissociation of cancer cells from the primary tumor and colonization of new tumor at distant organ. Cell migration and invasion play as the key early steps and required actin reorganization and extracellular matrix (ECM) degradation to achieve cell metastasis. The inhibition of these behaviors is an intriguing approach to minimize cancer metastasis. Erianthridin, a phenolic compound isolated from the Thai orchid *Dendrobium formosum* exhibits several pharmacological activities; however, the effect of erianthridin on lung cancer cell metastasis has not been observed. In this study, we demonstrated that non-toxic and non-proliferative concentrations of erianthridin was able to attenuate cell migration and invasion by disruption of actin stress fibers and lamellipodia formation. The mRNA level of MMP-2 and MMP-9, the matrix-degrading protease, were significantly decreased in a dose-dependent manner after erianthridin treatment. Mechanistic investigation revealed that the active form of Akt and its downstream effectors mTOR and p70^{S6K} were strongly suppressed in the presence of erianthridin. In addition, an in-silico study revealed that erianthridin bound directly at the ATP-bonding site of Akt with both hydrogen bonding and van der Waals interaction, resulting in dephosphorylation of Akt. This study provides preclinical information of erianthridin which exhibits a promising anti-metastasis activity against lung cancer.

Field of Study: Pharmacology and
Toxicology

Student's Signature

Academic Year: 2020

Advisor's Signature

ACKNOWLEDGEMENTS

Frist of all, I would like to express my deep and sincere gratitude to my advisor, Associate Professor Varisa Pongrakhananon, Ph.D., for her expert advice, encouragements, constant guidance and supporting, which have given me throughout this project. These helpfulness and kindness are really appreciated.

My earnest thanks to Associate Professor Boonchoo Sritularak for providing erianthridin from his laboratory to be use in this project. Without his kindness, this project could not be accomplished.

I express my deep sense of gratitude to Department of Pharmacology and Physiology, Faculty of Pharmaceutical Sciences, Chulalongkorn university for offering all facilities to carry out this project.

I extended my sincere thanks to my thesis committee Associate Professor Suree Jianmongkol, Ph.D., Visarut Buranasudja, Ph.D., and Kriengsak Lirdprapamongkol, Ph.D. for advantage suggestion for enhance the coverage of thesis.

Finally, The Scholarship from the Graduate School, Chulalongkorn University Graduate Scholarship to Commemorate the 72nd Anniversary of His majesty King Bhumibol Adulyadej, the 90th Anniversary of Chulalongkorn University Fund (Ratchadapiseksomphot Endowment Fund), and from Overseas Research Experience Scholarship for Graduate Students is gratefully acknowledged.

Sutthaorn Pothongsrisit

TABLE OF CONTENTS

	Page
ABSTRACT (THAI).....	iii
ABSTRACT (ENGLISH).....	iv
ACKNOWLEDGEMENTS.....	v
TABLE OF CONTENTS.....	vi
LIST OF TABLES.....	ix
LIST OF FIGURES.....	x
LIST OF ABBREVIATIONS.....	12
CHAPTER I.....	14
INTRODUCTION.....	14
1.1 Background and rationale.....	14
1.2 Objectives.....	16
1.3 Hypothesis.....	16
1.4 Benefits of the study.....	16
1.5 Keywords.....	16
CHAPTER II.....	17
LITERATURE REVIEWS.....	17
2.1 Lung cancer.....	17
2.2 Cancer metastasis.....	20
2.2.1 Epithelial to mesenchymal transition (EMT).....	21
2.2.2 Cell migration.....	24
2.2.3 Cell invasion.....	32

2.2.4 Anoikis resistance and metastatic colonization.....	34
2.3 The PI3K/Akt/mTOR signaling pathway in metastasis.....	34
2.4 Erianthridin.....	37
CHAPTER III.....	38
MATERIALS AND METHODS.....	38
3.1 Materials and Equipment.....	38
3.1.1 Cell lines and culture.....	38
3.1.2 Chemicals and Reagents.....	38
3.1.3 Equipment.....	40
3.2 Experimental design.....	41
3.3 Methods.....	42
3.3.1 Erianthridin preparation.....	42
3.3.2 Cell viability assay.....	42
3.3.3 Cell proliferation assay.....	42
3.3.4 Transwell migration assay.....	43
3.3.5 Wound healing assay.....	43
3.3.6 Transwell invasion assay.....	44
3.3.7 Anchorage-independent growth assay.....	44
3.3.8 Immunofluorescence assay.....	45
3.3.9 RNA extraction, cDNA synthesis and quantitative real-time PCR (qRT-PCR)	46
3.3.10 Western blot analysis.....	47
3.3.11 Small interference RNA Transfection assay.....	49
3.3.12 Molecular docking.....	49

3.3.13 Statistical analysis.....	50
3.4 Conceptual framework.....	51
CHAPTER IV	52
RESULT.....	52
4.1 Cytotoxicity of erianthridin on non-small cell lung cancer cells.....	52
4.2 Effect of erianthridin on non-small cell lung cancer cell proliferation	53
4.3 Erianthridin inhibits human non-small cell lung cancer cell migration	54
4.3 Erianthridin inhibits human non-small cell lung cancer cell invasion	56
4.4 Erianthridin inhibits an anchorage-independent growth of human non-small cell lung cancer cells.....	58
4.5 Erianthridin suppresses TGF- β -induced migration and anchorage-independent growth of human non-small cell lung cancer cells	60
4.6 Erianthridin suppresses actin stress fibers and lamellipodia formation through Rac1-dependent pathway.....	63
4.7 Erianthridin inhibits <i>MMP-2</i> and <i>MMP-9</i> expressions in non-small cell lung cancer cells.....	66
4.8 Erianthridin suppresses cell migration and invasion in an independency of EMT process.....	68
4.9 Eriathridin attenuates Akt/mTOR/p70 ^{S6K} signaling pathway	70
4.10 Eriathridin possible binds to Akt and inhibits Akt activity.....	73
CHAPTER V	76
DISCUSSION.....	76
REFERENCES	91
VITA.....	93

LIST OF TABLES

	Page
Table 1 List of primers used in quantitative real-time PCR (qRT-PCR)	47
Table 2 List of antibodies used in western blot analysis	48
Table 3 List of siRNA used in small interference RNA transfection assay	49



LIST OF FIGURES

	Page
Figure 1 Cancer incidence and mortality worldwide. The charts show the distribution of incidence and mortality for the common cancer worldwide	17
Figure 2 The different types of lung cancer are described histologically	19
Figure 3 5-Year relative survival by stage at diagnosis of lung and bronchus cancer.	20
Figure 4 The transition of epithelial cells to mesenchymal phenotype was induced by the growth factors or tumor microenvironment	22
Figure 5 Cancer cells migrate in a lamellipodium-dependent manner with actin polymerization at the front edge, and actin contractility at the rear	26
Figure 6 Rho GTPases family signaling pathway. The three major Rho GTPases family, Cdc42, Rac1, and Rho, are activated by guanine-nucleotide exchange factors (GEF) to regulate actin reorganization	31
Figure 7 The PI3K/Akt/mTORC1 signaling pathway. Activated Akt phosphorylates various substrates that perform different functions including several cytoskeleton-regulating proteins and epithelial-mesenchymal transformation (EMT)-activating proteins that specifically regulate cell motility.....	36
Figure 8 The structure of erianthridin (3,4-dimethoxy-9,10-dihydrophenanthrene-2,7-diol).....	37
Figure 9 Cytotoxicity of erianthridin on non-small-cell lung cancer cells.....	52
Figure 10 Effect of erianthridin on non-small cell lung cancer cell proliferation.....	53
Figure 11 Erianthridin inhibits cell migration of non-small cell lung cancer cells.....	55
Figure 12 Erianthridin inhibits human non-small cell lung cancer cell invasion.....	57
Figure 13 Erianthridin inhibits an anchorage-independent growth of human non-small cell lung cancer cells.....	59

Figure 14 Erianthridin suppresses TGF- β -induced migration and anchorage-independent growth of human non-small-cell lung cancer cells.	62
Figure 15 Erianthridin suppresses actin stress fibers and lamellipodia formation through Rac1-dependen pathway.....	65
Figure 16 Erianthridin inhibits <i>MMP-2</i> and <i>MMP-9</i> expression of non-small cell lung cancer.....	67
Figure 17 Erianthridin suppresses cell migration and invasion in an independency of EMT process.....	69
Figure 18 Erianthridin inhibits cell migration and invasion via an Akt/mTOR/p70 ^{S6K} -dependent mechanism.	72
Figure 19 Erianthridin directly binds to Akt.....	75
Figure 20 A Scheme diagram of this study. Erianthridin suppresses lung cancer cell migration and invasion through inhibition of Akt/mTOR/p-p70 ^{S6K} signaling pathway...	80

LIST OF ABBREVIATIONS

%	=	percentage
mM	=	millimolar
μ M	=	micromolar
μ L	=	microliter
Akt	=	protein kinase B
ATP	=	adenosine triphosphate
CTC	=	circulating tumor cell
DMEM	=	Dulbecco's modified Eagle's medium
ECM	=	extracellular matrix
EGF	=	epithelial growth factor
EMT	=	epithelial to mesenchymal transition
FBS	=	fetal bovine serum
FGFR	=	fibroblast growth factor receptor
GAPs	=	GTPase-accelerating proteins
GEFs	=	guanine nucleotide exchange factors
LE	=	ligand efficiency
LIMK	=	Lim kinase
MLC	=	myosin light-chain
MMP	=	matrix metalloproteinase
MT-MMP	=	membrane type-matrix metalloproteinase
mTOR	=	mammalian target of rapamycin
NMII	=	non-muscle myosin II
NSCLC	=	non-small cell lung cancer
p70 ^{S6K}	=	p70 S6 kinase
PAK	=	p21-activated kinase

PDB	=	protein data bank
PDK1	=	pyruvate dehydrogenase kinase
PI3K	=	phosphoinositide 3-kinase
RMSD	=	root-mean-square deviation
RPMI	=	Roswell park memorial institute
ROCK	=	Rho-associated coiled-coil forming kinase
SCLC	=	small cell lung cancer
siRNA	=	small interference RNA
TF	=	transcription factor
TGF- β	=	transforming growth factor beta



CHAPTER I

INTRODUCTION

1.1 Background and rationale

Lung cancer is one of the most frequently diagnosed cancer, and approximately 80%-85% of all lung cancer patients are classified into non-small cell lung cancer (NSCLC) (1). Chemotherapy, radiation therapy or surgery are primary options for an early stage non-small cell lung cancer, however recurrence of disease often occurs after multimodality treatment which develop to an advanced stage (metastasis) of lung cancer (2). The prognosis of patients with advanced stage remains poor due to metastatic progression by which the 5-year survival rate accounts for less than 6% (3). Therefore, inhibition of metastasis is one of the potential approaches to improve patient outcome. Lung cancer metastasis occurs through a multistep process that involves with the dissemination of lung cancer cells from primary tumor to distant organs. Loss of cellular adhesion is an initial step of metastatic cascade to facilitate a migratory phenotype in which epithelial to mesenchymal transition (EMT) is reported as important mechanism behind cancer cell dissociation (4). Following the transition, metastatic cells can migrate and invade individually or as an assembly of multiple cells through extracellular matrix (ECM) and then enter the vascular system to form secondary tumors at distant organ (5). Various studies had been reported that cell migration and invasion are the critical steps for metastasis, and the blockage of these steps was shown to suppress cancer metastasis (6).

Actin cytoskeleton plays a crucial role in cell migration and invasion by distinct mechanisms. First, the polymerization of actin at the leading edge provides the formation of protrusive structures including lamellipodia and filopodia for attaching at the new surface and generating force to drive cell movement (7). In

addition to the membrane protrusion formed, the force is produced by actin stress fiber that initiated through actin and myosin II filaments to build contractile system in the cells (8). The Rho family of small GTPase including Cdc42, Rac1 and Rho A is important regulator for the actin rearrangement. The Cdc42-GTP and Rac1-GTP, an active form of Rho GTPase family, are able to activate Arp2/3 complex leading to induce the actin polymerization and formation of lamellipodia, whereas the active Rho-GTP form is responsible for the formation of actin stress fibers through regulation of Rho-associated coiled-coil forming kinase (ROCK) activities (9). Moreover, the degradation of surrounding tissue also occurs during metastasis and increases movability of cancer cells to disseminate to secondary sites. Matrix metalloproteinases (MMPs) are responsible for degradation of ECM by which MMP-2 and MMP-9 closely related to tumor invasiveness and poor prognosis in patients (10).

Several signaling pathways have been reported to govern these alterations including protein kinase B (Akt)/the mammalian target of rapamycin (mTOR) signaling pathway (11). The phosphorylated Akt stimulates the downstream effectors including mTORC1 and p70 S6 kinase (p70^{S6K}) and cytoskeleton proteins. It was found that active p70^{S6K} is able to bind directly with F-actin that can rearrange the actin cytoskeletal through cross-linking and stabilizing filaments by inhibition of cofilin-induced actin depolymerization (12). In addition, active p70^{S6K} promotes Rac1 and Cdc42 activation leading to polarized actin structure and directed cell migration (13). Furthermore, Akt/mTOR/p70^{S6K} signaling pathway is associated with the regulation of MMPs expression, especially MMP-2 and MMP-9 (10, 14). Targeting at Akt signaling pathway are therefore promising approaches for an attenuation of cancer metastasis.

Currently, therapeutic interventions mostly focus on localized cancer than migrating cells, and repetitive treatments potentially mediated cancer aggressiveness phenotypes. Many affords have been made to discover alternative therapeutic interventions, and natural compounds exhibit promising pharmaceutical activities.

The phenolic compounds derived from Thai orchid (*Dendrobium* spp.) display anti-cancer properties such as gigantol, moscatilin and cyripedin (15-17). Recently new compound, erianthridin, isolated from *Dendrobium formosum* exhibits various pharmacological activities such as anti-inflammatory and vasorelaxant, however the effect of erianthridin on cancer metastasis remained unknown (18, 19). Therefore, this study aims to investigate the potential effect of this compound on metastatic behaviors of lung cancer focusing on cell migration and cell invasion and its underlying mechanisms.

1.2 Objectives

1. To investigate the inhibitory effect of erianthridin on metastatic behaviors of non-small cell lung cancer focusing on cell migration and cell invasion.
2. To investigate the molecular target of erianthridin on metastatic process in non-small cell lung cancer.

1.3 Hypothesis

Erianthridin has the *in vitro* inhibitory effect on human non-small cell lung cancer cell metastasis through AKT/mTOR/ p70^{S6K}-mediating cell migration and invasion.

1.4 Benefits of the study

Erianthridin is able to inhibit non-small cell lung cancer cell migration and invasion that plays a key early event in the metastatic process. Therefore, erianthridin has a potential to develop into an anti-cancer drug, providing a new approach for the treatment of metastatic lung cancer.

1.5 Keywords

- Erianthridin
- Cell migration and invasion
- Protein kinase B
- Actin stress fibers
- Lamellipodia
- Mammalian target of rapamycin

CHAPTER II

LITERATURE REVIEWS

2.1 Lung cancer

Lung cancer is a malignant tumor that caused by an uncontrolled growth of abnormal cells in lung tissue. Some of lung cancer cells can break away from the primary site, invade to nearby lymph vessels or blood vessels and enter to systemic circulation. The circulating tumor cells can move to other parts of the body and colonize at the secondary site to form new tumor (4). This process is known as metastasis of cancer which is the leading cause of death among the patients with lung cancer. According to cancer statistics, the lung cancer is the main cause of cancer incidence and mortality. Approximately 2.1 million (11.6%) of new lung cancer case is diagnosed worldwide that is the highest incidence of cancer types (Figure 1). Similarly, lung cancer is represented to be the first cause of common cancer deaths globally with about 1.8 million (18.4%) deaths (Figure 1) (1). Tobacco smoking is the greatest risk factor that associated to lung cancer. It is accounting for 80% of lung cancer deaths. Other risk factors are pollution, air quality and genetic risk factors (20).

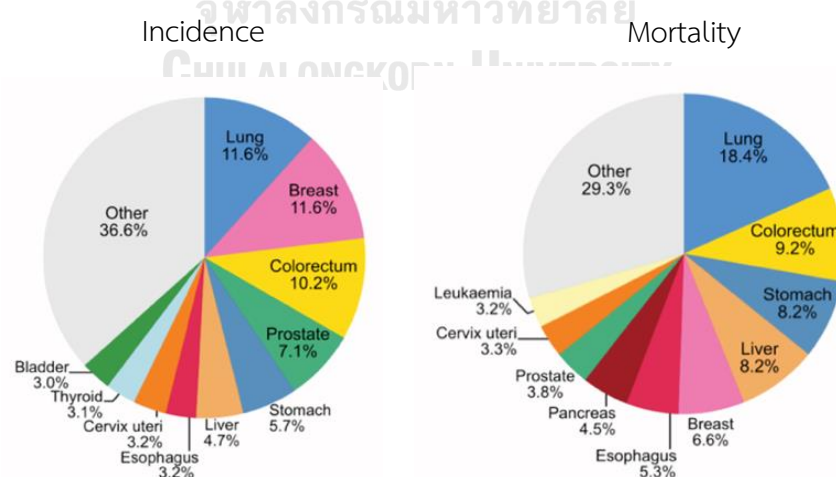


Figure 1 Cancer incidence and mortality worldwide. The charts show the distribution of incidence and mortality for the common cancer worldwide(1).

Types of lung cancer can be categorized into two groups by microscopic appearance of lung cancer cells. Small cell lung cancers (SCLC) are an aggressive type which has rapid growth and early development of metastases. However, the patients with small cell lung cancer accounts for 15-20% of lung cancer cases and have highly response rate with chemotherapy compared to other types of lung cancer (21), where about 80-85% of patients are diagnosed with non-small cell lung cancer (NSCLC) (22). Non-small cell lung cancer can be classified into three major groups including lung adenocarcinoma, squamous cell lung carcinoma and large-cell lung carcinoma (Figure 2).

- Lung adenocarcinoma is the most common type which accounts for 40% of lung cancers. This type of lung cancer can be found mainly in non-smokers and smoke.
- Squamous cell lung carcinoma is responsible for 25-30% of all lung cancers. This type of lung cancer tends to be linked with a history of smoking. It often locates at the bronchi of lung tissue or spreads to surrounding tissue such as lymph nodes.
- Large cell lung carcinoma is the less common type of non-small cell lung cancer. About 10-15% of all lung cancers is large-cell lung carcinoma. This type is similar to small cell lung cancers which has rapid growth rate and spread quickly to distant parts of the body.

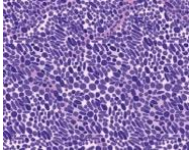
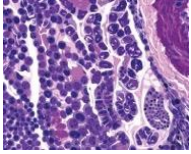
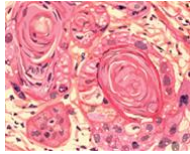
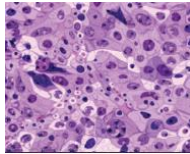
Small cell lung cancer cell	Non-small cell lung cancer cell		
	Lung adenocarcinoma	Squamous cell lung carcinoma	Large cell lung carcinoma
			

Figure 2 The different types of lung cancer are described histologically

For early stage of non-small cell lung cancer (stage I or stage II), the surgery is the first-line treatment for resectable non-small cell lung cancer. Chemotherapy, targeted therapy, or combinations are usually used to prevent the relapse of lung cancer. For stage III or stage IV of lung cancer, chemotherapy or targeted therapy is the main treatment for cancer. However, about 30-70% of patients have a recurrence with metastatic cancer after complete treatment course which is majority of mortality. The 5-year survival rate for stage IV lung cancer during 2009-2015 is approximately 6% which is lower than other stages of lung cancer (Figure 3) (3). Therefore, new treatment options including new compounds, immunotherapy and cancer vaccine are being developed for patients with metastatic lung cancer to improve clinical outcome.

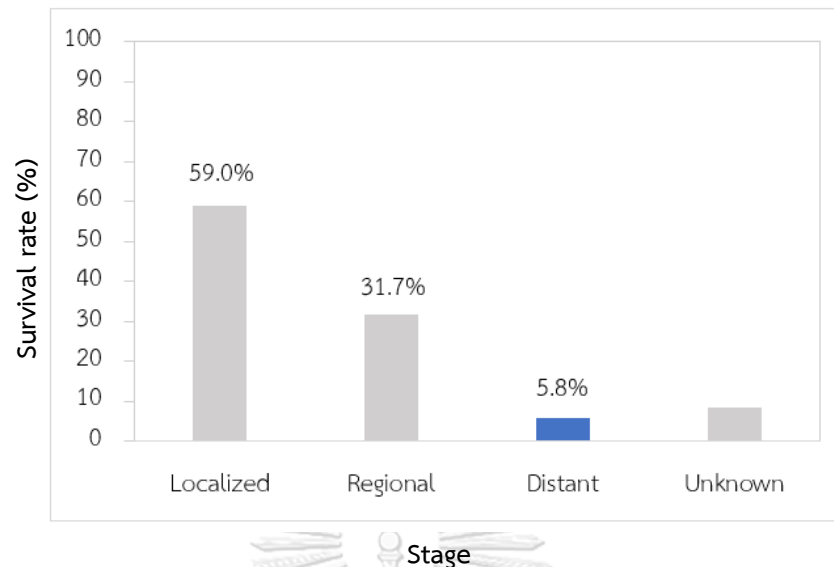


Figure 3 5-Year relative survival by stage at diagnosis of lung and bronchus cancer (3).

2.2 Cancer metastasis

Cancer metastasis occurs through the multi-step process which cancer cells escape from the primary site and spread to other areas of the body for the formation of new tumors. To leave the primary tumor, tumor cells lose their cell-cell and cell-matrix adhesion capacity and detach from the primary tumor. The change in cell-matrix interactions allow tumor cells to migrate and invade through surrounding tissues. This process involves the secretion of matrix metalloproteinases (MMPs) to degrade extracellular matrix (ECM). Following, these steps can help tumor cells penetrate the endothelium and the basement membrane into circulatory system, becoming circulating tumor cells (CTCs). CTCs are able to survive and spread through blood vessels until they arrest at the distant organ site and establish a new tumor. The metastasis cascade is therefore dependent on cell migration and invasion which results in the dissociation of tumor cells from primary site (4).

2.2.1 Epithelial to mesenchymal transition (EMT)

The epithelial-mesenchymal transition (EMT) is one of the crucial steps to mediate cancer metastasis. During EMT process, epithelial cells which are connected by adhesion molecule on their lateral membrane undergo several biological changes that enable them to become mesenchymal cells with increased migratory capacity and invasiveness (23). EMT is recognized by a loss of epithelial markers such as E-cadherin, claudin and cytokeratin, followed by upregulated the mesenchymal markers such as N-cadherin, vimentin, and fibronectin (Figure 4).

- **Cell-surface marker of EMT:** E-cadherin is one of the cell adhesion molecules (CAM) which is expressed in epithelial cells. It has an important role in the formation of adherence junctions of cells with each others. Several studies reported that E-cadherin expression is often decreased during EMT which lead to loss of cell polarity and epithelial phenotypes. Many factors were found to regulate E-cadherin expression. Hypermethylation at the E-cadherin promotor were known as a main mechanism to downregulate the transcription of E-cadherin gene, causing cancer metastasis. Snail transcription factor is also shown to suppress E-cadherin expression by the direct binding of Snail to E-cadherin promotor. Src tyrosine kinase were found to regulate the level of E-cadherin by post-translation mechanism. Activated Src can phosphorylate E-cadherin which initiate the endocytosis of E-cadherin, resulting in a decrease of E-cadherin distribution on epithelial cells. Therefore, restoring of E-cadherin could be a potential approach to suppress tumor metastasis (24, 25).

N-cadherin, a marker of ongoing EMT, typically expressed at low levels in normal epithelial cells but it is highly upregulated in several types of carcinoma. Crosstalk of N-cadherin with other membrane proteins such as

fibroblast growth factor receptor (FGFR) activates Rho GTPase family to promote migration and invasion in mesenchymal cells. Furthermore, it also activates MAPK signaling pathway and enhances stemness properties in cancer cells (26). Therefore, the acquisition of N-cadherin appears to be a critical step during cancer metastasis.

- **Cytoskeleton markers of EMT:** Vimentin is the intermediate filament protein and often found in the cytoplasm of mesenchymal cancer cells. Several studies had been demonstrated that vimentin was able to interact with actin cytoskeletons and microtubules to maintain mechanical integrity in the cells. In addition, vimentin also mediated the structure of actin cytoskeleton by organizing actin fibers or microtubules to generate driving forces for cell motility (27, 28).

β -catenin is a cytoplasmic plaque protein that plays essential function during EMT process. Normally, β -catenin is located at the cell membrane of epithelial cells, and it links cadherin to cytoskeleton in the cells (29). In cells undergoing EMT, β -catenin dissociates from E-cadherin and translocates to the nucleus that promotes the expression of EMT-related gene (28).

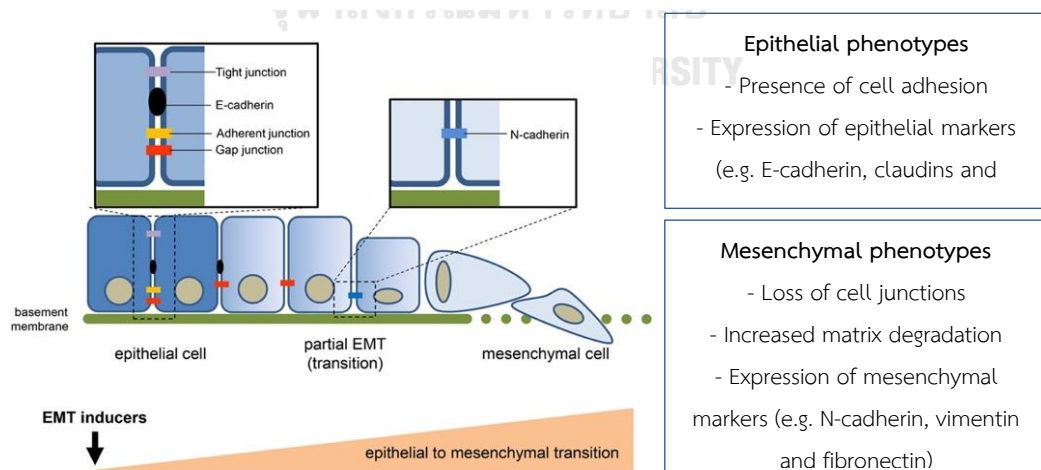


Figure 4 The transition of epithelial cells to mesenchymal phenotype was induced by the growth factors or tumor microenvironment(30).

For induction of EMT process, the various cytokines including growth factors (TGF- β , EGF) and hypoxia are required to induce the EMT program (31, 32). They are able to trigger EMT-associated transcription factors (TFs) to suppress the expression of epithelial markers and increase the expression of mesenchymal markers in cancer cells. Various studies had been indicated that the Snail, ZEB, and Twist are the major families of transcription factors for control EMT program in cancer cells.

- **Snail:** The two members of the Snail family of transcription factors, Snail1 and Snail2 (Slug) that are known as zinc finger transcription factor. They interact directly to E-box elements in the E-cadherin promoter that can suppress cell adhesion molecule (30, 33). In addition to these transcription factors, they upregulate expression of mesenchymal markers (vimentin, fibronectin) and matrix metalloproteinase (MMPs), a group of enzymes in extracellular matrix degradation, which enhance invasive and metastatic properties of cancer cells (34). The multiple signaling pathways are involved to modulate snail and slug including serine/tyrosine receptor induces the expression of snail, the Wnt pathway promotes Snail stability and the PI3K/AKT/mTOR pathway modulating Snail nuclear transport and ubiquitin-mediated degradation (35).
- **ZEB:** There are two subtypes of ZEB family including ZEB1 and ZEB2 (SIP1). Zinc finger transcription factors have a high affinity for E-cadherin promoter. The binding of TFs leads to repress E-cadherin transcription, thereby disruption of cell interaction (36). The several EMT-inducing signals pathway such as inflammatory cytokine, TGF- β signaling have been implicated in regulating activation of ZEB family via PI3K/Akt pathway (37). Hypoxia can also modulate ZEB TFs via interaction between HIF1 α and ZEB1 promoter (38).

- **Twist:** Twist families including Twist1 and Twist2 are basic helix-loop-helix transcription factors by which Twist1 plays role in regulating the EMT process (30). Twist1 decreases transcription of E-cadherin indirectly because it lacks ability to bind to E-box of E-cadherin promotor. However, various studies have shown that elevation Twis1 expression which is associated with invasiveness and metastasis of cancer cells (39).

In addition, there are crosstalk among ZEB, Snail and Twist families in cellular signaling. For example, slug activates ZEB1 through binding to ZEB1 promotor. Snail also maintains the stability of Twist1 that can cause activation of Snail2. These interactions are responsible for promoting mechanism of epithelial to mesenchymal transition (40).

2.2.2 Cell migration

Once the tumor cells dissociate from the solid tumor *via* EMT process, tumor cells have to migrate across the extracellular matrix or surrounding tissue for long distances to escape from the primary tumor. Cell migration is initiated by the formation of actin rich structures to generate contractile force and adhere to the new area during migration. According to loss of cells-cell junction, the actin nucleation protein that localized at cell context is released and move to the leading edge of cells. The actin polymerization at the leading edge enhances cancer cells to form the protrusive structure including lamellipodia and filopodia (9). These events enable cancer cell elongation and directional migration. Then, cell can move forward by actin contractility at the cell rear (Figure 5). However, lamellipodia and filopodia have markedly different in actin architectures and signaling pathway regulated their formation.

- **Lamellipodia:** Lamellipodia, the sheet-like membrane protrusions, are composed of a branched of actin filament network, and found at the leading edge of motile cells. The formation of lamellipodia is commonly triggered by Arp2/3 complex to establish the branched of actin network which is stabilized by cortactin (actin-binding protein). During migration, tumor cells extend this protrusive structure to attach to the new site and generate pulling force for cell movement (7).
- **Filopodia:** Filopodia, the finger-like membrane protrusions, contains a bundled parallel of actin filament and is also found at the leading edge of cells or the front of lamellipodia (41). Fascin has been reported to be an important actin-cross linking protein in filopodia to maintain the elongation of filament for pushing the membrane (42).

Within the cell body, the actin polymerization promotes the formation of actin stress fibers which are the major contractile structures in the migrating cells. Actin stress fibers are composed of bundles of actin, non-muscle myosin II (NMII) and various cross-linking proteins such as α -actinin. To push the cell forward, NMII head attaches to the actin filaments forming the cross-bridge. The interaction between NMII and actin filaments results in a release of ADP and change the conformation of NMII leading to the contraction of actin bundles (8, 43).

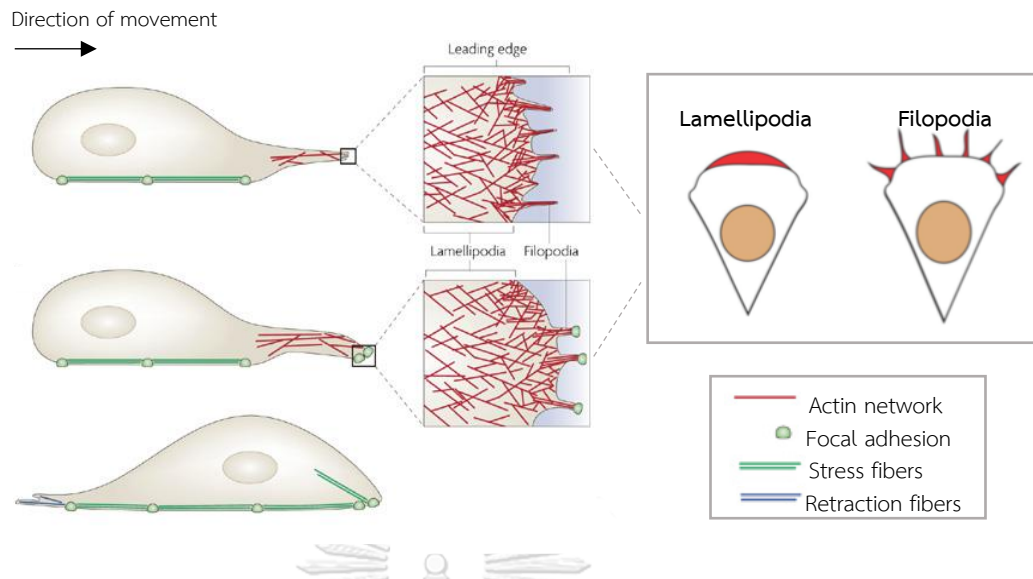


Figure 5 Cancer cells migrate in a lamellipodium-dependent manner with actin polymerization at the front edge, and actin contractility at the rear(44, 45).

Members of the Rho GTPase families are key regulators of cellular morphology, actin dynamics and cellular adhesion. The Rho GTPase families can be classified into 8 subfamilies including Rac subclass (Rac1, Rac2, Rac3, RhoG), Rho subclass (RhoA, RhoB, RhoC), Cdc42 subclass (Cdc42, RhoQ, RhoJ), RhoUV subclass (RhoU, RhoV), RhoBTB subclass (RhoBTB1, RhoBTB2, RhoBTB3), Rnd subclass (Rnd1, Rnd2, Rnd3), RhoH subclass and RhoF subclass (RhoD, RhoF) (9). Overactivation of Rho GTPase members especially Cdc42 Rac1 and RhoA can be found in metastatic cancer (46). Activation of Rac1 induces lamellipodia formation whereas activation of Cdc42 induces filopodia formation that promote migration of cancer cells (47). Activated RhoA enhances cancer cell motility by inducing actin polymerization and contraction. To trigger Rho family proteins, Guanine-nucleotide exchange factors (GEFs) is stimulated target proteins by exchanging of GDP-bound to GTP-bound form of proteins, while GTPase-activating proteins (GAPs) hydrolyses GTP-bound and turn to an inactive form (47). The activated Rho family proteins stimulate downstream effector proteins as follows (Figure 6)

- **RhoA-dependent pathway:** The GTP-binding protein RhoA binds to the pleckstrin homology domain of ROCK Kinase I and ROCK kinase II (ROCKI, ROCKII) releasing an autoinhibitory loop within ROCK. Activated ROCKI and ROCKII translocate from cytosol and localize on the plasma membrane to phosphorylate their substrates including myosin light chain (MLC) and LIM Kinase (LIMK) (37). Phosphorylation of MLC promotes actin polymerization and contraction whereas phosphorylation of LIMKs leads to phosphorylate cofilin resulting in inhibition of actin depolymerization.
- **Rac1-dependent pathway:** The GTP-binding protein Rac1 bind to and stimulate serine-threonine kinases p21-activated kinases (PAK). After binding, PAK is autophosphorylated and phosphorylate LIMK to inhibit cofilin activity (48). To initiate the lamellipodia formation, the Rac1-GTP directly interact with the WAVE complex, resulting in a dissociation of the complex into two subcomplexs including WAVE-HSPC300 and PIR121-Nap125-Abi2 complex. WAVE and HSPC300 complex has been reported to be an essential activator of Arp2/3 complex which is required to nucleate branched actin network for lamellipodia formation (49).
- **Cdc42-dependent pathway:** The GTP-binding protein Cdc42 activates WASP or N-WASP through binding with a specific region on WASP or N-WASP. The activated WASP or N-WASP also stimulates Arp2/3 complex resulting in filopodia formation of cells (50).

As mentioned above, Rho GTPases families show an important role in cancer metastasis based on their function in actin remodeling. For this reason, targeting Rho GTPase is an interesting therapeutic approach to improve the survival of patients with metastatic disease.

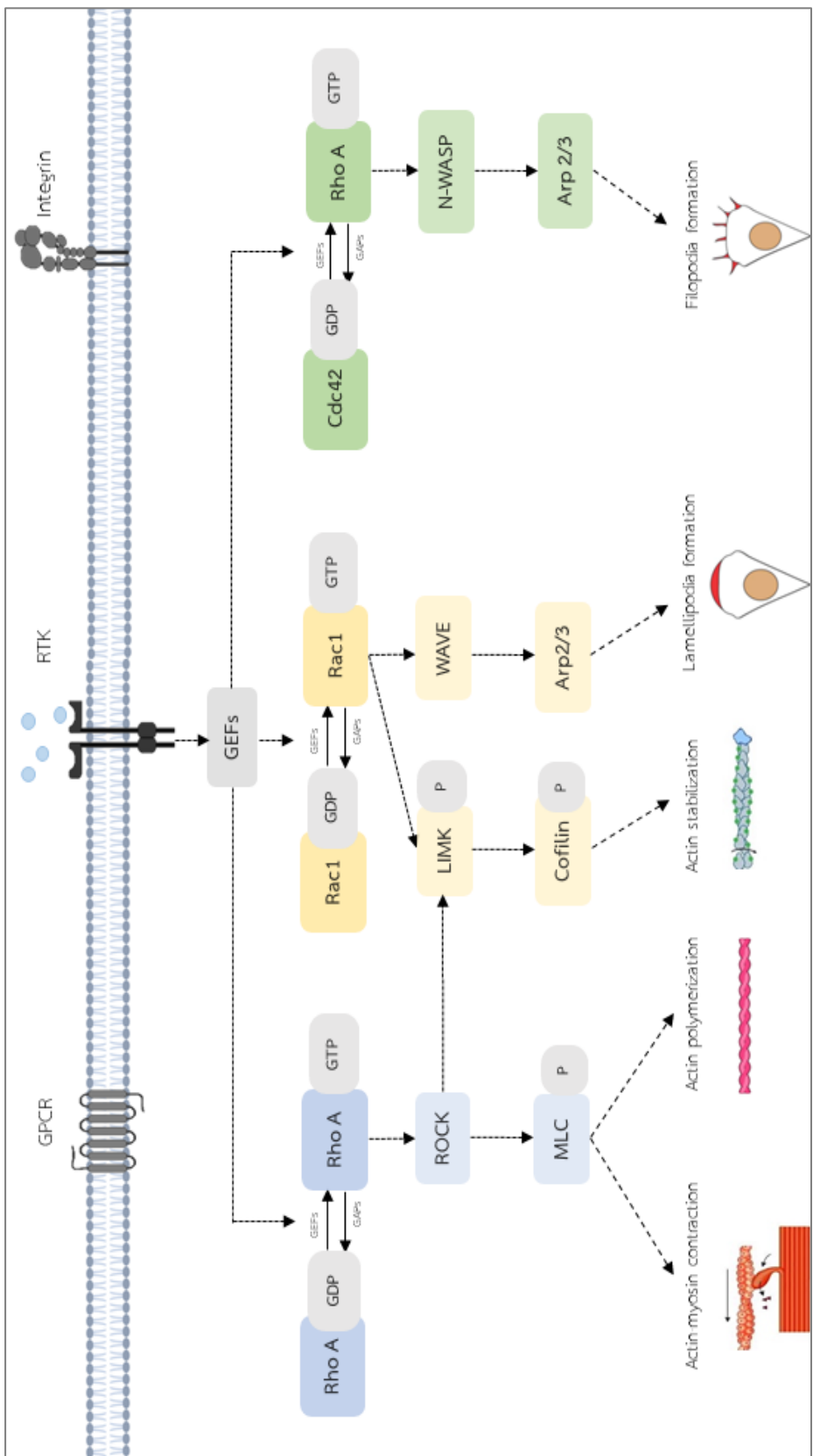


Figure 6 Rho GTPases family signaling pathway. The three major Rho GTPases family, Cdc42, Rac1, and Rho, are activated by guanine-nucleotide exchange factors (GEF) to regulate actin reorganization(9, 45).

2.2.3 Cell invasion

The extracellular matrix (ECM) is a network of macromolecules that contains several components including fibers (collagen, laminin and fibronectin), proteoglycans, glycoproteins and polysaccharides (hyaluronic acid) (51). It plays a crucial role for providing structural support for surrounding cells. In cancer, the extracellular matrix act as a barrier impeding movement of cancer cells into nearby tissue or blood vessels. However, invading cancer cells are able to penetrate the ECM by degradation with proteolytic enzymes (Matrix metalloproteinase: MMPs) and escape from the primary tumor site.

MMPs are a member of extracellular proteinase which consist of two conserved motifs. One motif is catalytic domain with a zinc ion required for enzyme activity. The other retained motif is a cysteine-containing pro-domain which maintains the inactive state of MMPs. MMPs can be classified into five major groups based on their structure and substrates specificity including collagenases, gelatinases, stromelysins, matrilysins and membrane-type MMPs (MT-MMPs) (52)

- **Collagenases:** MMP-1, MMP-8 and MMP-13 are able to cleave fibrillar collagen type I, II, III, IV and XI; however, MMP-1 cannot degrade the basement membrane components. Overexpression of MMP-1 has been detected in bladder cancer and related to a poor prognosis in patients, as well as in patients with gastric and breast cancer (53). MMP-13 has been found to slightly promote cell invasion, but it has an important role in angiogenesis of tumor cells. Upregulation of MMP-13 initiates capillary tube formation both *in vivo* and *in vitro* model (54).
- **Gelatinase:** MMP-2 (Gelatinase A) and MMP-9 (Gelatinase B) are responsible for degradation of collagen type I and type IV which is abundant in basement membrane. Various studies have demonstrated that MMP-2 and MMP-9 are

often associated with tumor invasion and metastasis (52). Overexpression of MMP-2 is positively correlated with the number of lymph node metastasis and tumor size in *in vivo* model (55). MMP-9 is commonly up-regulated in various cancer cell lines and malignant tumor tissues, and increased MMP-9 expression can enhance the rate of cell metastasis to lymph node or distant organ (56). Inhibition of MMP-2 and MMP-9 result in a decrease cell motility and invasiveness and is a possible approach to improve the clinical outcomes in patients.

- **Stromelysins:** MMP-3, MMP-10, MMP-11 and MMP-12 are able to cleave fibrillar collagen type II, III, IV and XI. It has been found that MMP-3 functions as tumor promotor, facilitating cell proliferation and angiogenesis. MMP-11 is also highly expressed in various metastatic cancer cells, especially breast cancer. The level of MMP-11 expression is correlated with the poor prognosis in patient with breast cancer. Deletion of MMP-11 in mice are able to decrease tumorigenesis (52).
- **Matrilysins:** MMP-7 and MMP-26 can degrade only fibrillar collagen type I. Unlike most MMPs, MMP-7 usually expresses in many epithelial cells including liver, pancreases, epithelium of intestine and reproductive organ to control normal physiology process (52).

MT-MMPs: MT-MMPs can be subcategorize into type I transmembrane-type (MT1, MT2 MT3 and MT5-MMPs) and glycosylphosphatidylinositol-anchored type (MT4 and MT6-MMPs). Among them, MT1-MMP is closely related to tumor metastasis. MT-MMP has been shown to promote cell migration and invasion by cleavage the fibrillar collagen type I which is a major behavior during cell invasion. In addition, MT-MMP1 also stimulates epithelial growth factor receptor (EGFR) and induces cell migration via EGF-dependent pathway (57).

2.2.4 Anoikis resistance and metastatic colonization

Once metastatic cells have entered circulatory system. The most of cells in the absence of cellular adhesion are induced to mode of cell death via induction of anoikis. However, aggressive cancer cells are able to survive and circulate through blood vessels until they colonize at the secondary site by anoikis resistance (58). Mutation of the mitochondria death pathway, for example, overexpression of Bcl-2 family leads cancer cells to resistance to apoptosis (59). After that, metastatic cells extravasate from blood vessels, degradating of endothelium wall and transendothelial migrate to establish tumor at new organ (60).

2.3 The PI3K/Akt/mTOR signaling pathway in metastasis

The PI3K/Akt/mTOR axis is related to the maintenance of cancer cellular processes including cell survival and cell proliferation. However, several studies have shown that PI3K/Akt/mTOR pathway plays important role in cancer metastasis (61). Due to stimulation at tyrosine kinase receptor with growth factor, PI3K can generate the secondary messenger (PIP3) on the plasma membrane. After that, PIP3 bind to pleckstrin homology domain (PH) of Akt and lead to full activation of Akt via phosphorylated on Threonine 308 and serine 473 sites that mediated by PDK1 and mTORC2 respectively (62). Activated Akt can phosphorylates downstream effectors including mTORC1. mTOR is also a potent regulator in cancer cell migration and invasion. The mTOR has two different complexes including mTORC1 and mTORC2. Both mTORC1 and mTORC2 have crosstalk with PI3K/Akt pathway. mTORC1 is phosphorylated by activated Akt. In contrast to mTORC1, mTORC2 is the regulator of Akt through activation of Akt by phosphorylation (63). Activated Akt/mTOR pathway can affect downstream molecules including EMT-activating protein and cytoskeleton regulating protein (61).

Several studies have demonstrated that activation of the PI3K/Akt/mTORC1 axis drives the epithelial-mesenchymal transition program in various cancer cell lines (61). p70^{S6K} and 4E-BP1 are two essential downstream targets of the PI3K/Akt/mTORC1 axis. The mTORC1 activates p70^{S6K} by phosphorylation on threonine 389 site and then the active form of p70^{S6K} can stimulate expression of Snail that is a repressor of E-cadherin (64). The other downstream of mTORC1 is 4E-BP1 which is a family of translation repressor proteins. The non-phosphorylated form of 4E-BP1 binds tightly to the cap binding protein eIF4E. When mTORC1 phosphorylates 4E-BP1 on threonine 37/46, they can release eIF4E to bind with translation initiating components resulting in expression of Snail and MMP-9 (65). In addition, the PI3K/Akt/mTOR pathway functions as an upstream of Rho GTPase families to regulate the actin filaments. The activated-p70^{S6K} has been found to activate Rac1, cdc42 and their downstream leading cellular protrusion formation (12). Moreover, the activated-p70^{S6K} is able to bind directly with F-actin that can rearrange the actin cytoskeleton through cross-linking and stabilizing filaments by inhibition of cofilin-induced actin depolymerization (Figure 7) (13).

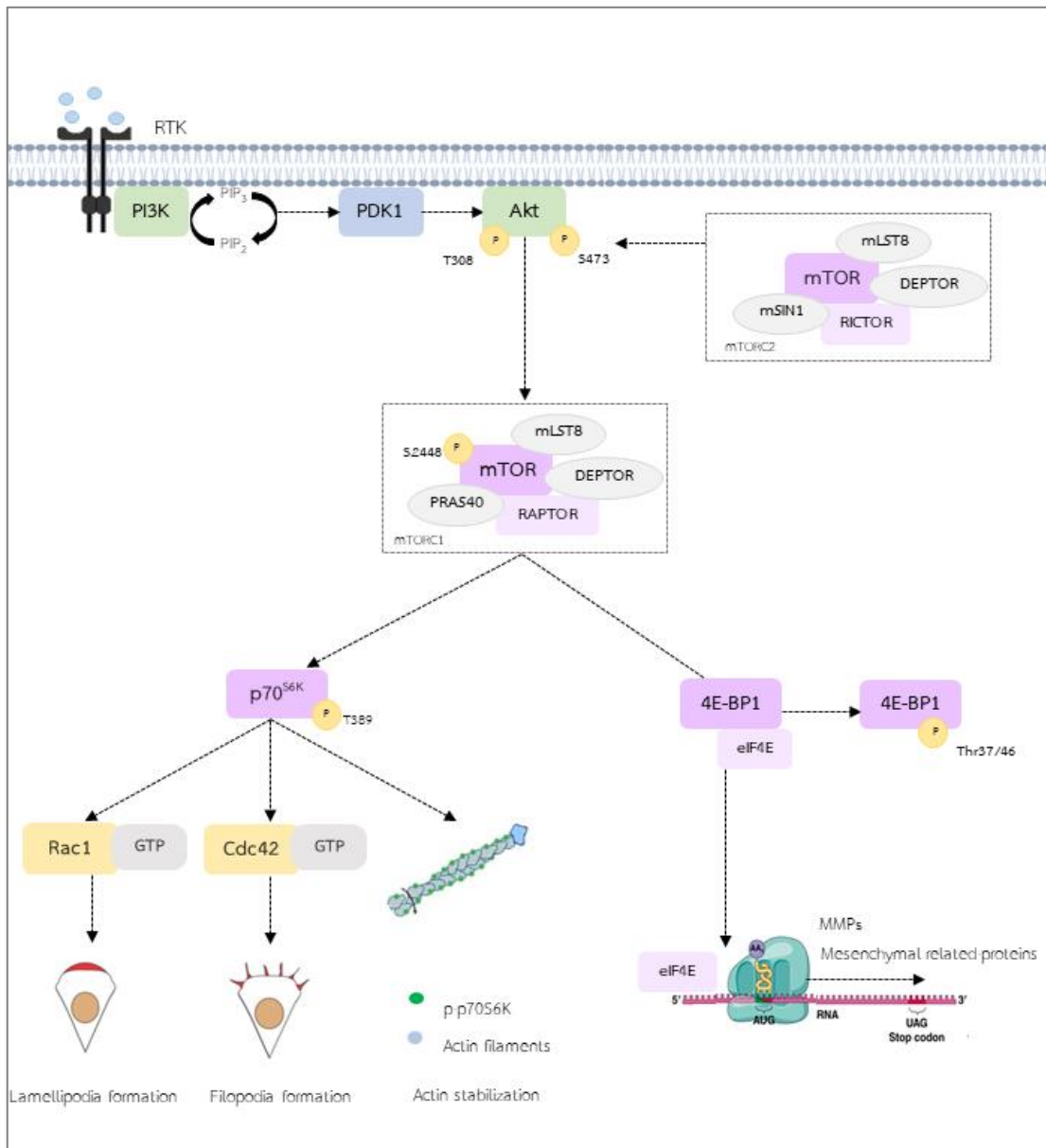


Figure 7 The PI3K/Akt/mTORC1 signaling pathway. Activated Akt phosphorylates various substrates that perform different functions including several cytoskeleton-regulating proteins and epithelial-mesenchymal transformation (EMT)-activating proteins that specifically regulate cell motility(11, 65).

2.4 Erianthridin

Erianthridin, 3,4-dimethoxy-9,10-dihydrophenanthrene-2,7-diol (Figure 8), is a phenolic compound that isolated from an extract of Thai orchid. *Dendrobium formosum* is a member of *Dendrobium* spp. that contains various biologically active substances including giganthol, moscatilin, cyripedin and erianthridin (3). Erianthridin is reported to have various pharmacological activities. Erianthridin demonstrates the inhibitory activity against superoxide anion generation and elastase release in human neutrophils that leads to inhibit inflammatory response mechanisms (18). Erianthridin can also have vasorelaxant activity in rat at 141.8 μM (19). Numerous studies indicated that the active compounds from *Dendrobium* spp. have anti-tumor activities in various tumor types. For example, giganthol has been shown to inhibit and induce apoptosis of HepG2 cells via the PI3K/Akt/NF- κB signaling pathway (66). Cyripedin can inhibit an epithelial-to-mesenchymal transition in non-small cell lung cancer cells via suppression of Akt/GSK-3 β signaling pathway (17). However, the effects of erianthridin in cancer cells have not been observed.

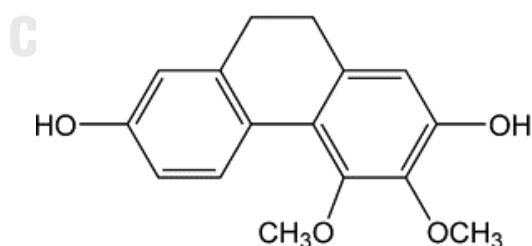


Figure 8 The structure of erianthridin (3,4-dimethoxy-9,10-dihydrophenanthrene-2,7-diol)

CHAPTER III

MATERIALS AND METHODS

3.1 Materials and Equipment

3.1.1 Cell lines and culture

Non-small cell lung cancer cell lines A549 and H460 were purchased from American Type Culture Collection (ATCC) (Manassas, VA, USA). H460 cells were cultured in Roswell park memorial institute (RPMI)-1640 medium. A549 cells were cultured in Dulbecco's modified Eagle's medium (DMEM). Both of medium were supplemented with 10% fetal bovine serum (FBS), 100 U/mL penicillin-streptomycin and 2 mM L-glutamine. Cells were maintained in a 37° C humidified incubator with 5 % CO₂.

3.1.2 Chemicals and Reagents

- **Cell culture reagents:** Roswell park memorial institute (RPMI) 1640 medium, Dulbecco's Modified Eagle Medium, L-glutamine, Penicillin/ Streptomycin, Fetal bovine serum (FBS), 0.25% Trypsin-EDTA and Phosphate-buffered saline (PBS) were purchased from GIBCO (Grand Island, NY, USA). Matrigel™ were obtained from Corning (Corning, NY, USA). Lipofectamine® RNAiMAX was purchase from Invitrogen (Carlsbad CA, USA).
- **Chemical reagents:** 3-(4,5-Dimethylthiazol-2-yl)-2,5-Diphenyltetrazolium Bromide (MTT) was purchased from Invitrogen (Carlsbad, CA, USA). Chloroform (CHCl₃) and hydrochloric acid (HCl) were purchased from Sigma (St. Louis, MO, Chemical, USA). Sodium chloride (NaCl), Boric acid (H₃BO₃), Sodium dodecyl sulfate (SDS), Ethanol, 2-propanol (Isopropanol) and Dimethyl sulfoxide (DMSO) were obtained from Merck Millipore (Billerica, MA, USA). Methanol

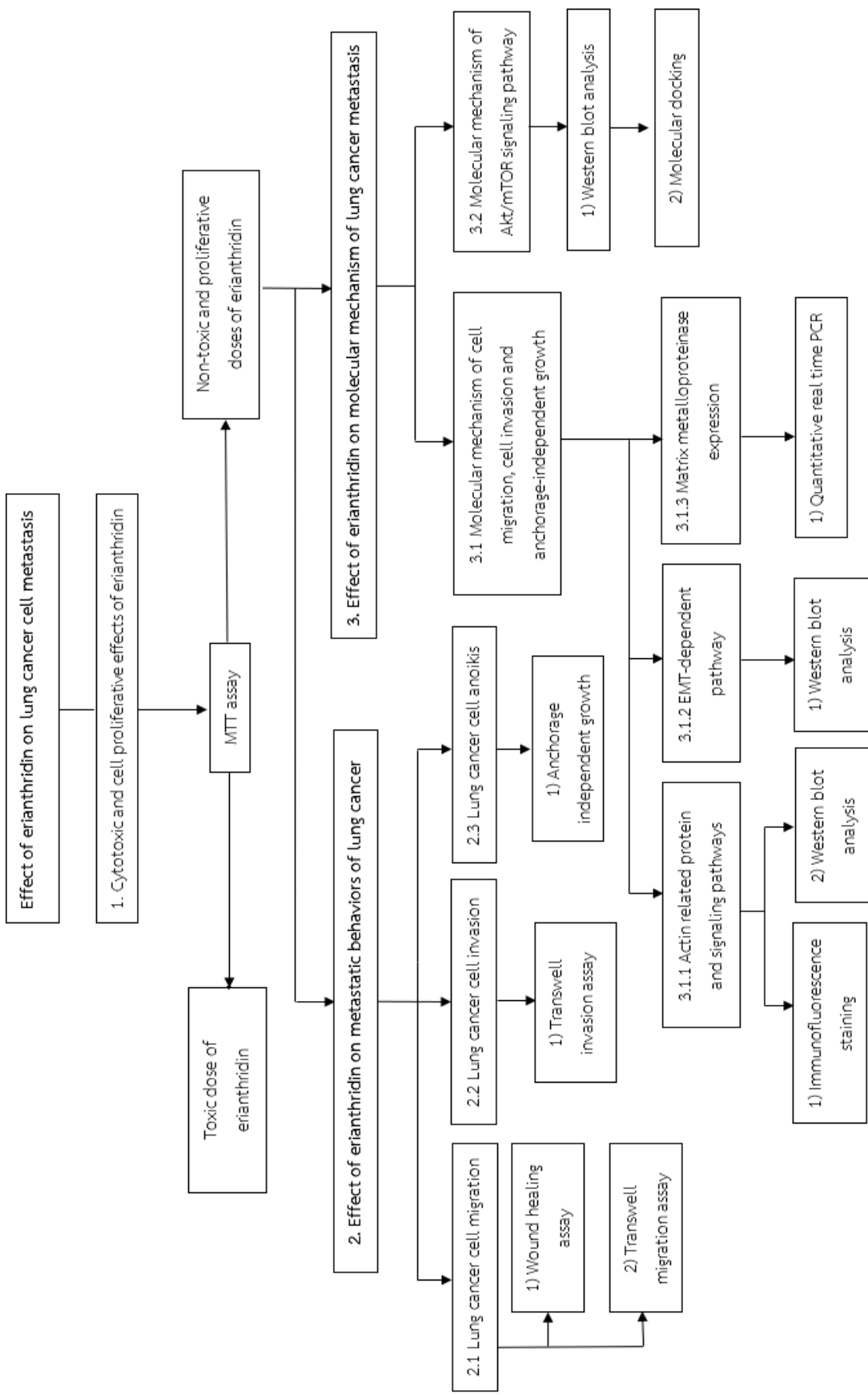
(CH₃OH) was purchased from Honeywell (S. Harvey, USA). Sodium bicarbonate (NaHCO₃) were obtained from Univar (Ajax Chemicals, AU).

- **Western blotting buffers and reagents:** BCA protein assay kits, Immobilon western chemiluminescent HRP substrate was purchased from Thermo Fisher Scientific Inc. (Waltham, MA, USA). AccuProtein Chroma (protein markers) was purchased from Enzmart (Enzmart Biotech, Thailand). Tetramethylethylenediamine (TEMED), 40% Acrylamide Solution were purchased from Bio-Rad Laboratories (Hercules, CA, USA). Skim milk powder for blotting was purchased from SERVA Electrophoresis GmbH (Heidelberg, Germany). Bovine serum albumin (BSA) was purchased from Nacalai tesque, Inc (Nakagyo-ku, Kyoto, Japan).
- **Primary and secondary antibodies:** Rabbit anti-Akt, rabbit anti-phosphorylated Akt, mTOR pathway antibody sampler kit, Epithelial-Mesenchymal Transition antibody sampler kit, mouse anti-GADPH, anti-rabbit IgG HRP-linked and anti-mouse IgG HRP-linked were purchased from Cell Signaling Technology (Beverly, MA, USA). RhoA/Rac1/Cdc42 activation assay kit was purchase from Cell biolabs, Inc. (SanDeigo, CA, US). Alexa fluor 568 phalloidin were purchased from Life Technologies (Eugene, OR, USA).
- **Real-Time PCR Reagent and kits:** GENEzol reagent was purchased from Geneaid Biotech (Shijr, New Taipei, Taiwan). SuperScriptTM III Reverse Transcriptase and Oligo(dT)₂₀ Primer were purchased from Invitrogen (Carlsbad, CA, USA). 2x SensiFASTTM SYBR[®] No-ROX Kit was purchased from Biorline (Taunton, MA, USA).

3.1.3 Equipment

LUNA II Automated cell counter (Logosbio, South Korea), Laminar air flow cabinet (Bosstech, Bangkok, Thailand), Humidified incubator and Centrifuge (Thermo scientific, Waltham, MA, USA), Vortex mixer (Scientific industries, NY, USA), pH meter (SevenCompacts220), Fluorescence microscope (Nikon Inverted Microscope Eclipse Ti-U Ti-U/B, NY, USA), Microplate reader (Anthros, Durham, USA), Autopipette 0.2-2 μL 2-20 μL 20-200 μL and 1,000 μL (Harikul, Thailand), 6-well microplates, 24-well microplates, 96-well plates, 60-mm tissue culture dishes, 10-cm tissue culture dishes (Iwaki, Japan)





3.3 Methods

3.3.1 Erianthridin preparation

Erianthridin was provided by Associate Professor Boonchoo Sritularak (Department of Pharmacognosy and Pharmaceutical Botany, Faculty of Pharmaceutical sciences, Chulalongkorn University). Erianthridin was dissolved in dimethyl sulfoxide (DMSO) to make a 100 mM stock solution and store at -20°C. Working solution was prepared by dilution of stock solution in complete media. The final concentration of DMSO in each well did not exceed 0.1%, which showed no toxicity.

3.3.2 Cell viability assay

Cell viability was measured in H460 and A549 cells using the MTT assays. Cells (10^4 cells/well) were plated onto 96-well plates overnight and then were treated with various concentrations of erianthridin for 24, 48, 72 h. After the treatments, 10 μ L of MTT solution (5 mg/mL) was added to each well and incubated at 37°C for 3-4 h. After incubation, the medium was removed and replaced with 100 μ L of DMSO to dissolve formazan crystals. The intensity of solution was measured at 570 nm by microplate reader. The cell viability was calculated as follows:

$$\% \text{ Cell viability} = \frac{\text{average absorbance of treated group}}{\text{average absorbance of control group}} \times 100$$

3.3.3 Cell proliferation assay

H460 and A549 cells were plated in 96-well plates at a density of 2×10^3 cells/well and then incubated overnight at 37°C for cell attachment. Cells were treated with non-toxic concentration of erianthridin and allowed growth for 24, 48, 72 h. After the indicated incubation time, 10 μ L of MTT solution (5mg/mL) was added to each well and incubated at 37°C for 4 h. The intensity of solution was

measured an absorbance at 570 nm using microplate reader. Relative cell growth was calculated to represent cell proliferation at each time point as follows:

Relative cell proliferation =

$$\frac{\text{average absorbance of each group}}{\text{average absorbance of each group at the initial time of treatment}}$$

3.3.4 Transwell migration assay

H460 and A549 cells (5×10^4 cells/well) were seeded onto the upper chamber of 24-well transwell insert filled with serum free media, and 500 μL of media containing 10% FBS was added at the lower chamber. Cells were treated with the various non-toxic concentrations of erianthridin and allowed to migrate to the lower chamber for 18-20 h. After incubation time, the non-migrated cells at the upper chamber were removed by cotton swabs, the migrated cells at the underside were fixed with cold methanol at -20°C for 5 min, and stained with DAPI in the dark at room temperature for 10 min. The five random fields of migrated cells were photographed under a fluorescent microscope with magnification 100x. The number of migrated cells was counted and calculated as a relative migrated cell to the untreated group as follows:

$$\text{Relative migration level} = \frac{\text{average number of cells in each group}}{\text{average number of cells in control group}}$$

3.3.5 Wound healing assay

H460 and A549 cells were plated onto 96-well plates with 2×10^4 cells/well and incubated overnight. A 10 μL -micropipette tip was used to scratch cell attachment to generate wound space. Cell debris was removed and replaced with media containing 1% fetal bovine serum. Cells were treated with various non-toxic concentrations of erianthridin and allowed to migrate for 24, 48, 72 h. At the end of

incubation time, the wound spaces were photographed under a phase contrast microscopy and quantified area of a space using Image J software. Relative wound area was calculated at each time as follows:

Relative wound area =

$$\frac{\text{average wound space of each group at each time point}}{\text{average wound space of each group at the initial time of treatment}}$$

3.3.6 Transwell invasion assay

Cell invasion assay was performed by transwell chambers which are coated with Matrigel™ (10 µg/mL). H460 and A549 cells were resuspended in serum free media and seeded onto the upper chambers of 24-well transwell at a density 5×10^4 cells/well. The 500 µL of media containing 10% FBS was added to the lower chamber. Cells were incubated with various non-toxic concentrations of erianthridin and allowed to invade the Matrigel™ to the lower chamber for 20 h. The non-invasive cells were removed by cotton swabs, the invasive cells at the underside were fixed with cold methanol at -20°C for 5 min and then stained with DAPI in the dark at room temperature for 10 min. The five random fields of cells that penetrated through the Matrigel™ were captured under a fluorescent microscope with magnification 100x. The number of invasive cells were counted and calculated as relative invasive cells to the control group as follows:

$$\text{Relative invasion level} = \frac{\text{average number of invasive cells in treatment group}}{\text{average number of invasive cells in control group}}$$

3.3.7 Anchorage-independent growth assay

To evaluate the metastatic potential of lung cancer cells, anchorage-dependent growth was performed by maintaining the cells in soft agar. The 24-well plates were coated with complete media containing 0.5% agarose at room temperature for 30

min to form the bottom layer. After solidification, H460 and A549 cells were trypsinized and suspended in complete media containing 0.3% agarose and plated onto the bottom layer with 1,000 cells/well. Cells were treated with various non-toxic concentrations of erianthridin in 500 μ L complete media which was added on top of the upper layer of soft agar. The media was replaced every 3 d to prevent drying of agar. Cells were incubated in a 37 °C humidified incubator to form colonies for 10 d. At the end of treatment, the cell colonies were stained with 0.01% crystal violet for 30 min at room temperature and washed with deionized water. All colonies per well were imaged under a phase contrast microscope. The size (μ m) of the colonies were measured by ImageJ software.

3.3.8 Immunofluorescence assay

The effect of erianthridin on actin stress fibers and lamellipodia formation were performed by immunofluorescence assay. H460 and A549 cells were plated at a density of 2×10^3 cells/coverslip in 24 well-plates and treated with non-toxic concentration of erianthridin for 48 h. Cells were fixed with 4% formaldehyde in PBS for 20 min at room temperature in the dark, treated with 0.1% Triton-x in PBS for 10 min and blocked with 4% BSA at room temperature for 30 min. The solution was decanted and washed with PBS. Cells were incubated with phalloidin for 1 h at room temperature in the dark, removed the solution and washed the cells with PBS. The coverslips are stained with DAPI for 10 min, rinsed with deionized water and mounted with FluorSave. To investigate changes in the actin cytoskeleton, cells were imaged using a fluorescence microscope with magnification 200x. The number of actin stress fibers per cell and area of lamellipodia were analyzed and compared with control group.

Relative stress fiber (per cell) =

$$\frac{\text{average number of stress fibers in treatment group}}{\text{average number of stress fibers in control group}}$$

Relative lamellipodia area (per cell) =

$$\frac{\text{average area of lamellipodia in treatment group}}{\text{average area of lamellipodia in control group}}$$

3.3.9 RNA extraction, cDNA synthesis and quantitative real-time PCR (qRT-PCR)

To evaluate expression of matrix metalloproteinase, the enzyme participates in extracellular matrix degradation, H460 and A549 cells were treated with erianthridin for 48 h. TRIzol™ reagent was added to lyse the cells. After that lysate was centrifuged at 12,000 x g at 4°C for 5 min and the supernatant was collected. The supernatant was incubated with 200 μL chloroform per 1 mL of TRIzol™ for 5 min and then centrifuged at 12,000 x g at 4°C for 15 min. The upper phase containing RNA was transferred to new tube and isopropanol was added into aqueous for precipitation of RNA. The gel-like pellet containing RNA was resuspended in 75% ethanol and dried for 10 min. The RNA yield was determined using NanoDrop Microvolume Spectrophotometers. The RNA was reverse transcribed to cDNA by ProtoScript® II Reverse Transcriptase following the manufacture's protocol.

The qualitative real-time PCR was performed to measured matrix metalloproteinase (*MMP-2*, *MMP-9*) expression. The 500 ng of cDNA template, 2x SensiFAST™ SYBR® No-ROX Kit and primers (Table 1) were prepared to 20 μL of reaction mixture. Amplification was performed in an IO-RAD T100™ thermal Cycler

as followed: denaturation at 95°C for 30 sec, followed by 40 cycles at 95°C for 5 sec, annealing temperature based on each primer for 10 sec. The relative of gene expression was analyzed using $\Delta\Delta C_t$ method. Fold difference in treatment group relative to control group was calculated as follows:

$$\text{Fold-difference} = 2^{(-\Delta\Delta C_t)}$$

$$\Delta\Delta C_t = \Delta C_t \text{ treatment group} - \Delta C_t \text{ control group}$$

$$\Delta C_t = \text{Average } C_T \text{ of target gene} - \text{Average } C_T \text{ of GADPH}$$

Table 1 List of primers used in quantitative real-time PCR (qRT-PCR)

Names	Primer's sequence
<i>MMP-2</i>	F: 5'-GAA GTA TGG GAA CGC CGA TGG-3'
	R: 5'-TTG TCG CGG TCG TAG TCC TCA-3'
<i>MMP-9</i>	F: 5'-CCT GGA GAC CTG AGA ACC AAT C-3'
	R: 5'-CCA CCC GAG TGT AAC CAT AGC-3'
<i>GADPH</i>	F: 5'-ACA TCG CTC AGA CAC CAT G-3'
	R: 5'-TGT AGT TGA GGT CAA TGA AGG G-3'

3.3.10 Western blot analysis

H460 and A549 cells were seeded onto 60-mm culture dishes with 1×10^6 cells/dish and allowed cells to adhere overnight. The media was removed and replaced with media containing 1% FBS. Cells were treated with various non-toxic concentrations of erianthridin and incubated for 24 h. At the end of incubation, cells were lysed with TMEM lysis buffer containing 20 mM Tris-HCl pH 7.5, 1mM $MgCl_2$, 150 mM NaCl, 20 mM NaF, 1% octylphenoxypolyethoxyethanol (NP), 0.1 mM phenylmethylsulfonyl fluoride, 0.5% sodium deoxychlorate and protease inhibitor

cocktail on ice for 40 min. The supernatant was collected, and total protein was determined by BSA protein assay kit. Equal amounts of protein were divided and then heated with 6X sampling buffer for 5 min at 95°C for denaturation of proteins. The proteins were separated by SDS-polyacrylamide gels and electrotransferred onto polyvinyl difluoride (PVDF) membranes. The membranes were blocked with 5% skim milk in tris-buffered saline with Tween 20 (TBS-T) for 1 h. The membranes were incubated with primary antibodies (Table 2) at 4°C overnight. After incubation, the membranes were washed with TBS-T and probed with diluted secondary antibodies for 2 h at room temperature. The blots were visualized by enhanced chemiluminescence system using Immobilon Western chemiluminescent HRP substrate. Quantification of the band intensity of protein expression was performed using ImageJ software.

Table 2 List of antibodies used in western blot analysis

Primary antibodies	Dilution
Rabbit anti-phosphorylated Akt (S473)	1:1000
Rabbit anti-Akt	1:1000
Rabbit anti-phosphorylated mTOR (S2448)	1:1000
Rabbit anti-mTOR	1:1000
Rabbit anti-phosphorylated p70 S6 Kinase (Thr389)	1:1000
Rabbit anti-N-cadherin	1:1000
Rabbit anti-Slug	1:1000
Rabbit anti-Snail	1:1000
Mouse anti-Rac1	1:1000

3.3.11 Small interference RNA Transfection assay

Double-stranded small interfering RNA (siRNA) targeting Akt was used in this experiment (Table 3). For siRNA transfection, 1×10^6 cells per dish were plated on a 60-mm dish overnight and A549 cells were transfected with 200 nM siRNA against Akt. Lipofectamine[®] RNAiMAX and siRNA against Akt were diluted in opti-MEM[®] medium and incubated at room temperature for 5 min. After incubation, diluted Lipofectamine[®] RNAiMAX were added to diluted siRNA against Akt and incubated at room temperature for 15-20 min, the mixture was then added dropwise onto the cells. After incubation for 18 h, the cells were subjected to further experiments.

Table 3 List of siRNA used in small interference RNA transfection assay

siRNA	siRNA's sequence
Akt	sense: 5'-GGA GAU CAU GCA GCA UCG C -3'
	antisense: 5'- GCG AUG CUG CAU GAU CUC C -3'

3.3.12 Molecular docking

The X-ray crystal structure of Akt was retrieved from Protein Data Bank (PDB) with PDB ID 3MVH. The structure of ETD was drawn by ChemDraw Ultra 17.0 (PerkinElmer, Waltham, MA, USA). The MM2 forcefield was used to minimize the structure, and the Gasteiger charges were added to both ligands and protein template to create a supported format for molecular docking study. The molecular docking of ETD and Akt was performed by AutoDock4.2 (67), which genetic algorithm (GA) parameters included 100 GA runs, a population size of 150, a maximum of 10,000,000 evaluations, and a maximum of 27,000 generations as described in previous study (68). The 3D ligand conformations, aligned within 2.0 Å root-mean-square deviation (RMSD), were grouped as the same conformation clusters. The ligand conformations which have the highest cluster were analyzed for free binding

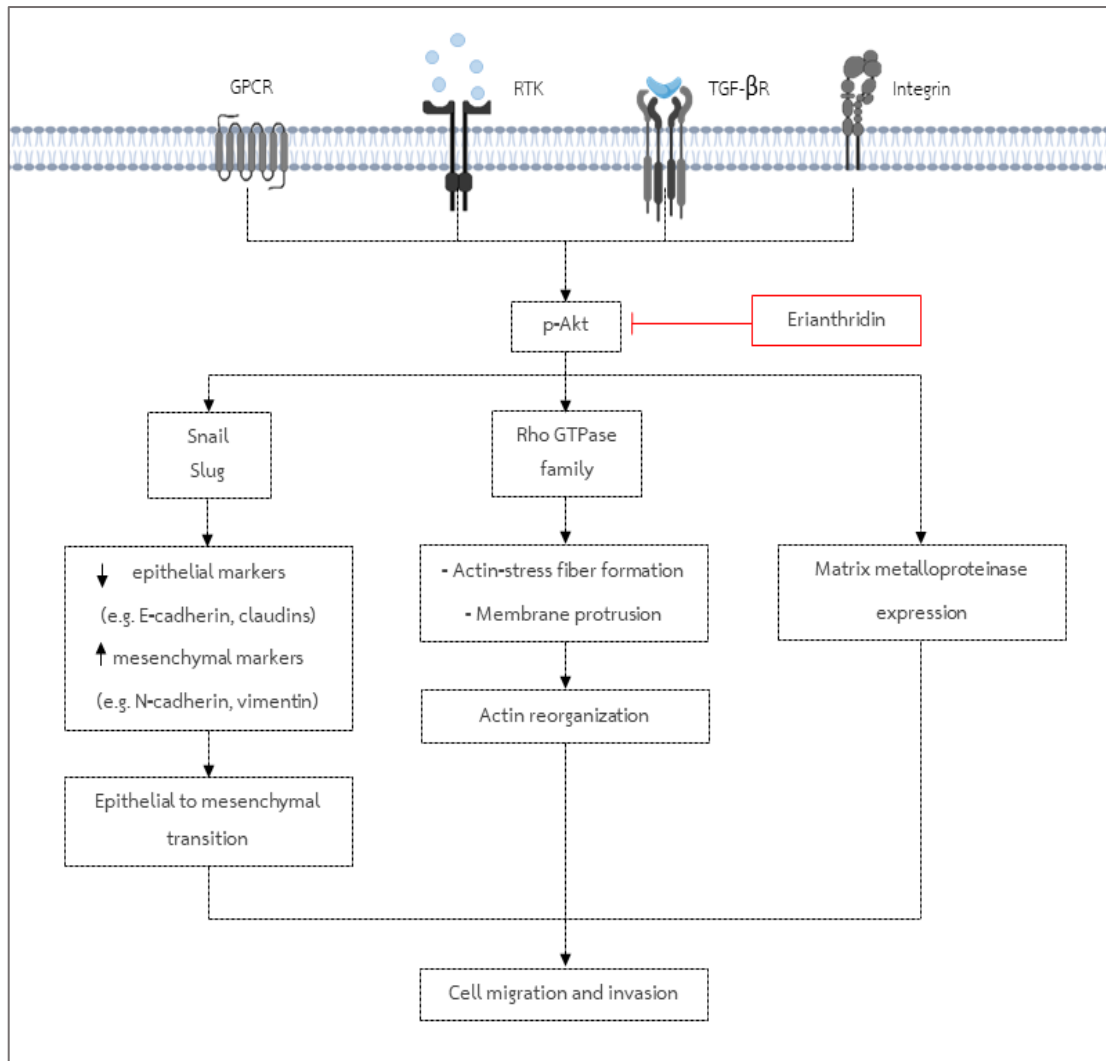
energies (ΔG) and ligand efficiency (LE). The binding interaction between ligands and target protein was analyzed by AutoDock4.2, PyMOL (Schrödinger, New York, NY, USA) and BIOVIA Discovery Studio Visualizer 2017 (Biovia, San Diego, CA, USA).

3.3.13 Statistical analysis

All data were reported as the mean \pm SEM that are performed at least three-independent experiments, and all data were analyzed using Prism 8 (GraphPad Software, Inc., San Diego, CA, USA). The student's *t*-test was used to analyze statistical differences between two groups. The One-way ANOVA with Tukey's Multiple Comparison Test was applied for determination the statistical significance between control and treatment groups. *P*-values less than 0.05 were considered statistically significance.



3.4 Conceptual framework



CHAPTER IV

RESULT

4.1 Cytotoxicity of erianthridin on non-small cell lung cancer cells

We first assessed the cytotoxic effect of erianthridin on lung cancer cells using MTT assay, the human lung cancer A549 and H460 cells were treated with various concentrations of erianthridin (0-500 μM) for 24, 48 and 72 h. As observed in Figure 9A-B, cell viability after treatment with erianthridin less than 50 μM did not show cytotoxic effect over incubation times in both types of lung cancer cells, whereas the higher concentration of erianthridin (≥ 100 μM) significantly reduced viable cells in a dose-dependent manner. Therefore, the concentrations of erianthridin lower than 50 μM were carried out in the next experiments to eliminate the interference of cytotoxic effect of compound on cell migration and invasion.

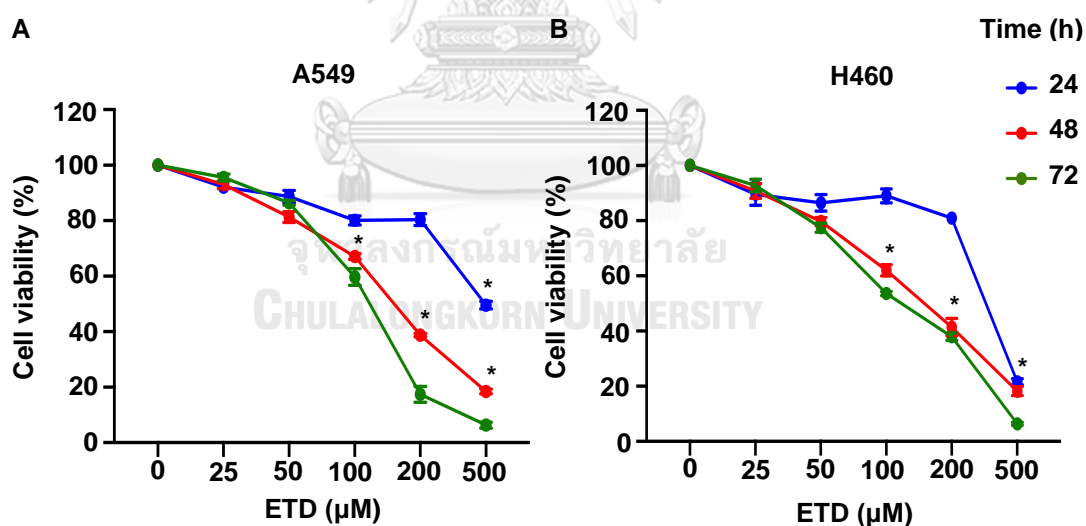


Figure 9 Cytotoxicity of erianthridin on non-small-cell lung cancer cells. (A) A549 and (B) H460 cells were treated with various concentrations (0-500 μM) of erianthridin for 24, 48 and 72 h. Cell viability was evaluated by MTT assay and represented as a percentage. The data are presented as mean \pm SEM ($n=3$). * $p < 0.05$ vs untreated control group.

4.2 Effect of erianthridin on non-small cell lung cancer cell proliferation

Since cell proliferation in response to erianthridin treatment can affect the investigation of metastatic capability, cell proliferation assay was performed using MTT assay to confirm that erianthridin had no effect on cell proliferation. Figure 10A-B shows that non-toxic dose of erianthridin (0-50 μ M) had no anti-proliferative activity for 24, 48 and 72 h in both A549 and H460 cells. Therefore, the concentrations of erianthridin lower than 50 μ M were used in the next experiments to eliminate the interference of proliferative effects of compound on cell migration and invasion.

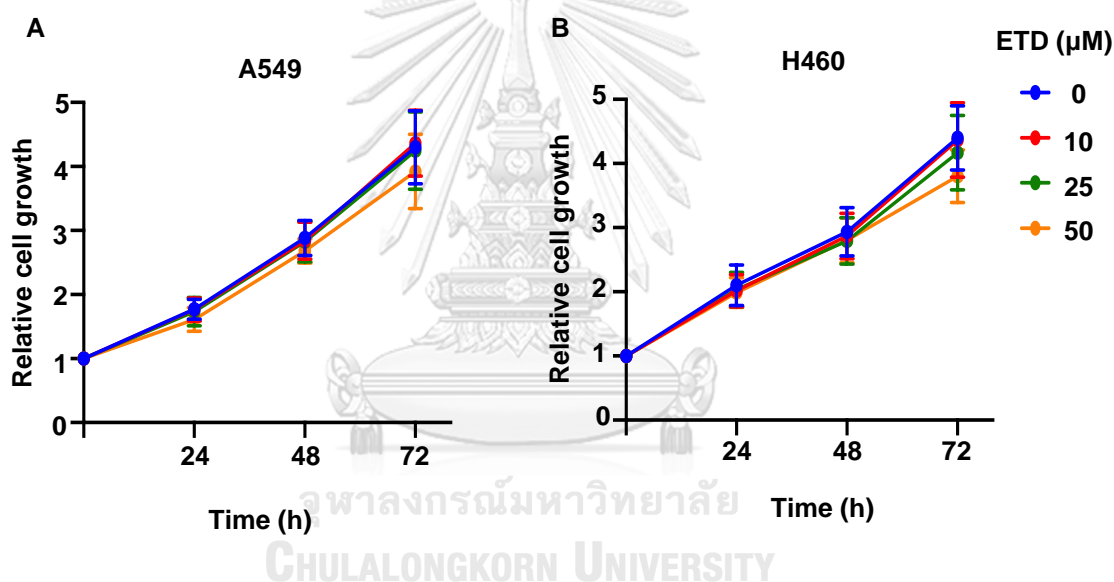
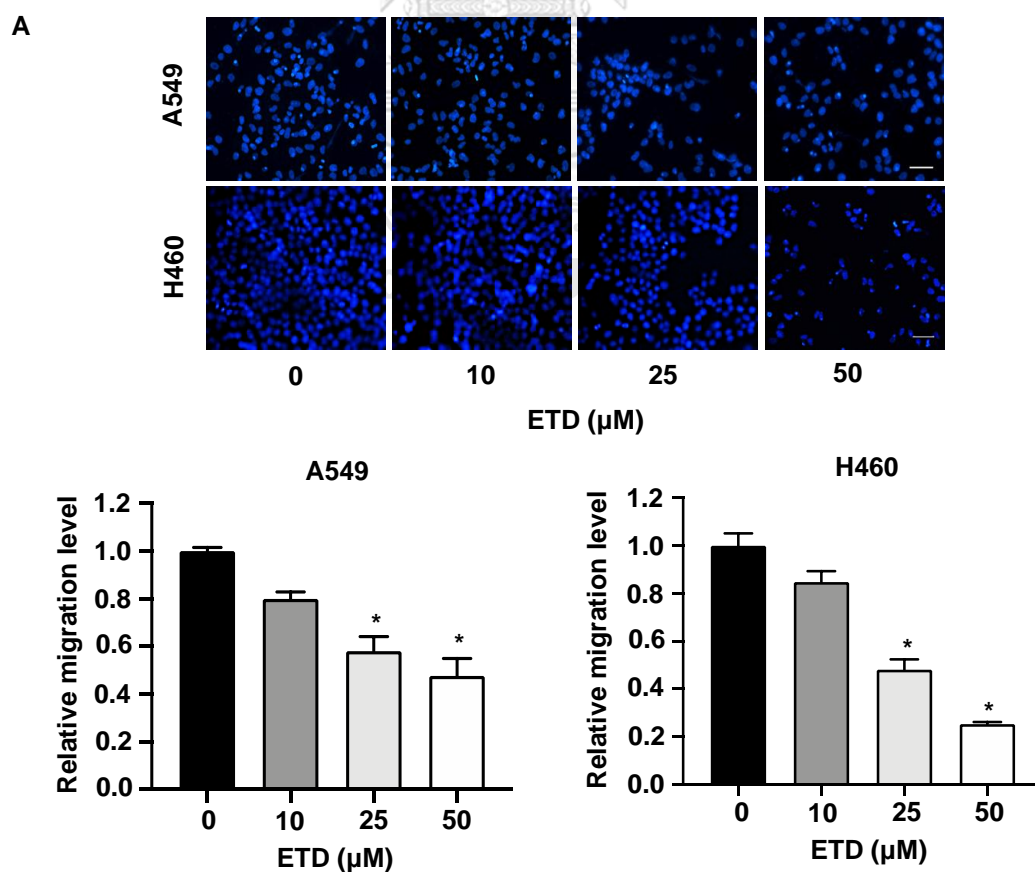


Figure 10 Effect of erianthridin on non-small cell lung cancer cell proliferation. (A) A549 and (B) H460 cells were treated with non-toxic concentrations (0-50 μ M) of erianthridin for 24, 48 and 72 h. Cell proliferation was evaluated by MTT assay. The rate of cell growth was calculated as value relative to time 0 h. The data are presented as mean \pm SEM (n=3). * p < 0.05 vs untreated control group.

4.3 Erianthridin inhibits human non-small cell lung cancer cell migration

During metastasis, cancer cells can move individually or collectively across the extracellular matrix or through the interstitial tissue (69). To evaluate whether erianthridin could suppress cell motility, transwell migration and wound healing assay were performed to determine the inhibitory effect of erianthridin on single and collective cell migrations, respectively. Transwell migration assay demonstrated that the number of migrated cells at the underside of membrane were clearly decreased in response to erianthridin treatment (Figure 11A). Consistently, the wound healing assay also revealed that erianthridin clearly decreased the migration ability in both A549 and H460 cells. Wound space remained largely when compared with control group after treatment with non-toxic doses of erianthridin, especially 50 μM (Figure 11B). These data suggest that erianthridin is an effective compound suppressing cell motility of lung cancer cells.



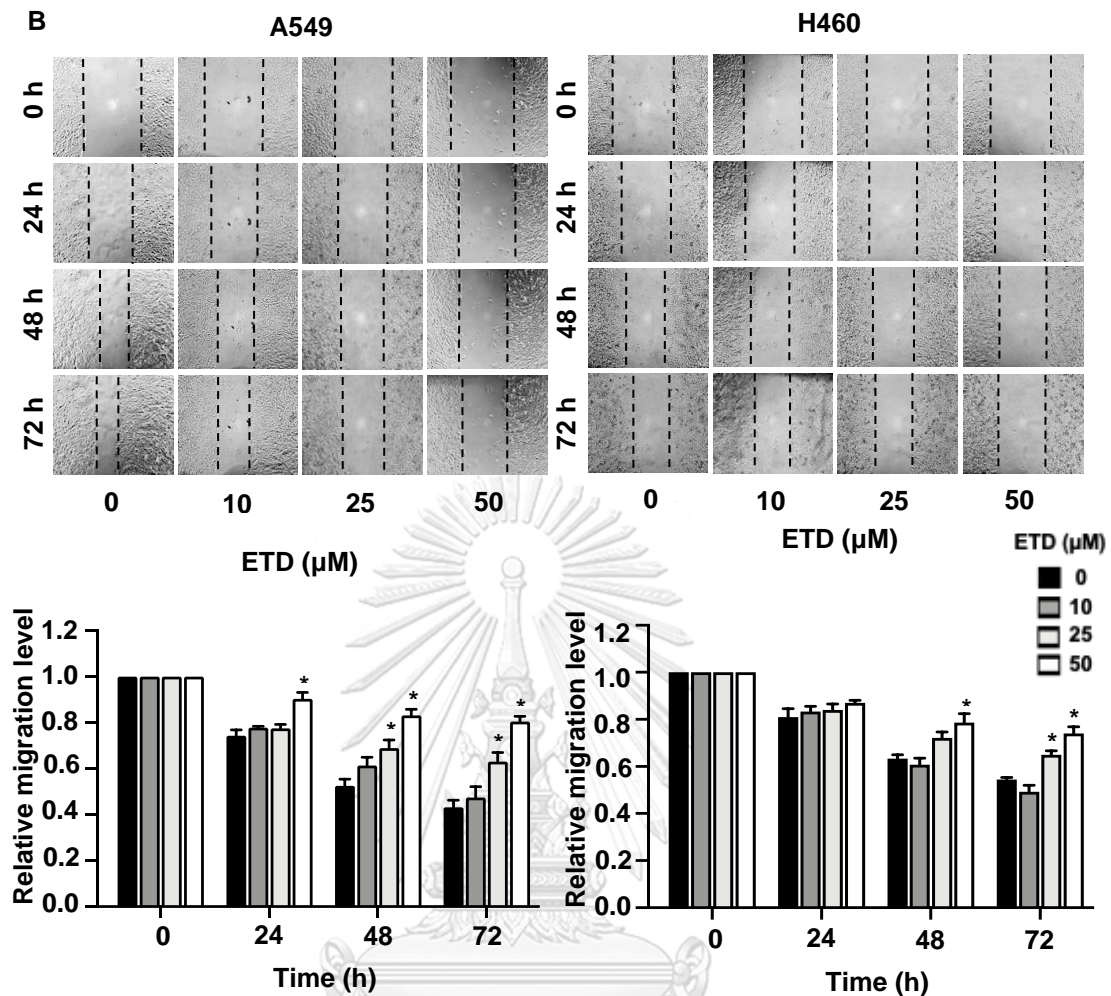


Figure 11 Erianthridin inhibits cell migration of non-small cell lung cancer cells.(A) A459 and H460 were seeded onto the transwell chamber and treated with non-toxic concentration of erianthridin (0-50 μM). After 20 h, the migrated cells were stained with DAPI and imaged by fluorescence microscopy. The cells on the lower side were analyzed as the relative number of migrated cells of treatment group compared to control group. Scale bar is 10 μm. (B) Monolayer of the cells was scratched with pipette tip to generate wound space and treated with 0-50 μM of erianthridin. The wound area was photographed under microscope at 0, 24, 48 and 72 h. The wound space was quantified as an area at each time point relative to an area at initial time point. All data are presented as mean ± SEM (n = 3). * $p < 0.05$ vs untreated control group.

4.3 Erianthridin inhibits human non-small cell lung cancer cell invasion

Cancer cell invasion is implicated as an important step facilitating cell dissociation from the solid tumor (70). To investigate the effect of erianthridin on the invasion of non-small-cell lung cancer cells, the transwell invasion assay was performed. After incubation, the results demonstrated that 25 and 50 μM of erianthridin extensively inhibited lung cancer cell invasion in both cell lines. As shown in Figure 12, the number A549 and H460 cells that penetrated through transwell membrane was obviously lower as compared with non-treatment group. These results suggest that erianthridin has an ant-invasive activity in human non-small-cell lung cancer cells.



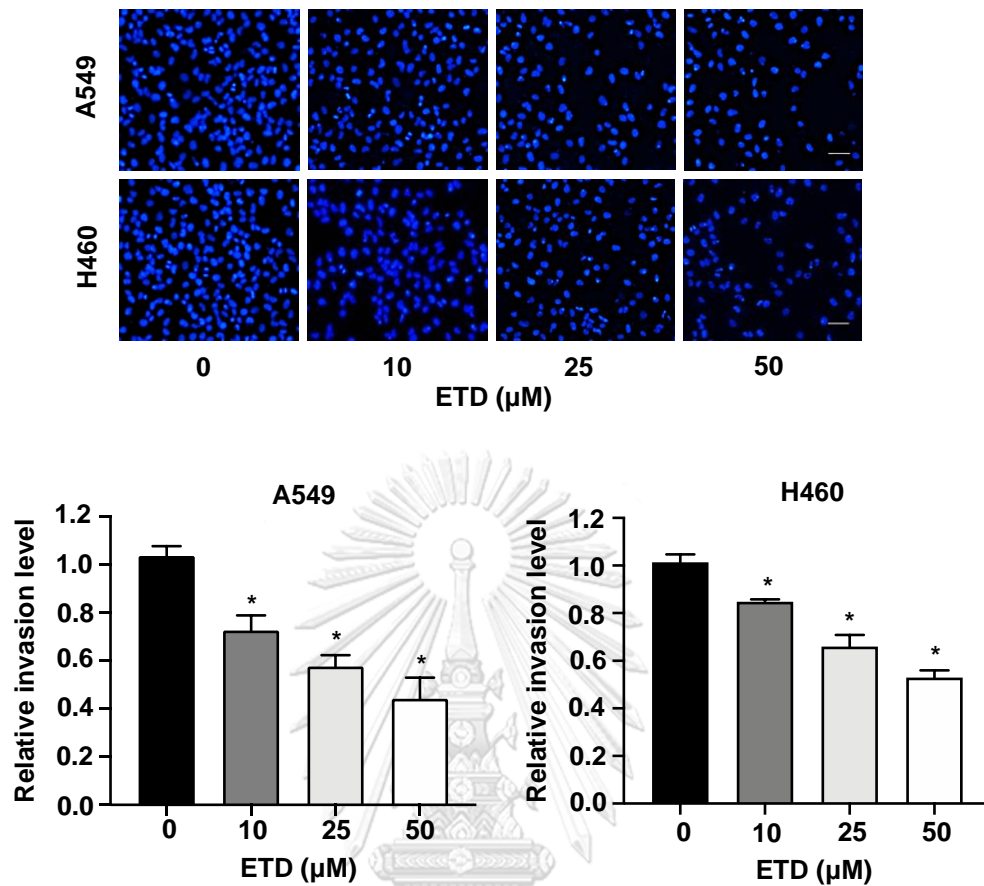


Figure 12 Erianthridin inhibits human non-small cell lung cancer cell invasion. A549 and H460 cells were seeded onto the transwell chamber coated with Matrigel™ and treated with non-toxic dose of erianthridin. After 20 h, the invaded cells were stained with DAPI and imaged by fluorescence microscopy. The cells on the lower side were analyzed as the relative number of invaded cells of treatment group compared to control group. Scale bar is 10 μm. The data are presented as mean ± SEM (n = 3). * $p < 0.05$ vs control group.

4.4 Erianthridin inhibits an anchorage-independent growth of human non-small cell lung cancer cells

Since cancer cells acquired survival mechanism to overcome cell detachment-induced apoptosis as established during systemic circulation (58). Colony formation in soft agar was performed to explore the effect of erianthridin on an anchorage-independent growth. As shown in Figure 13, colonies formed on soft agar were markedly smaller in response to erianthridin treatment in both cell lines, indicating that erianthridin was able to suppress an anchorage-independent growth in lung cancer cells.



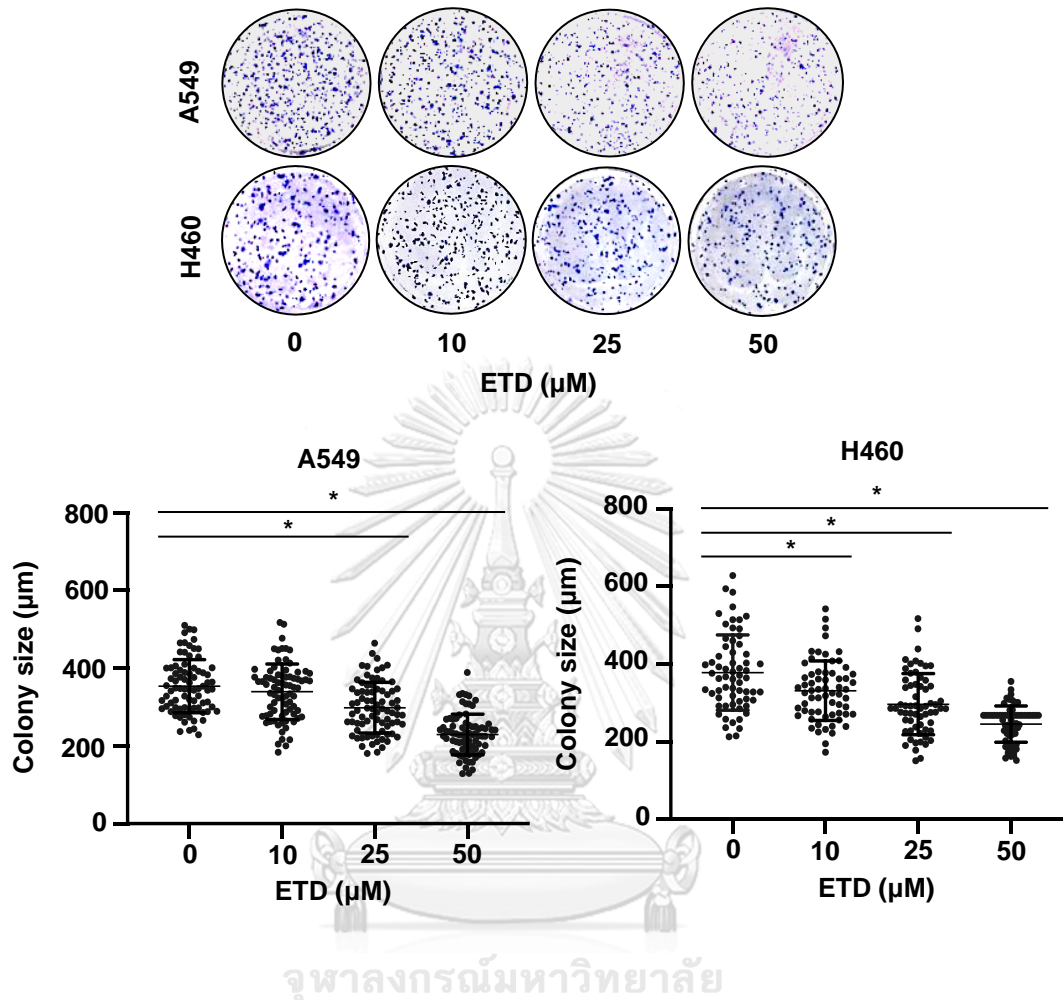
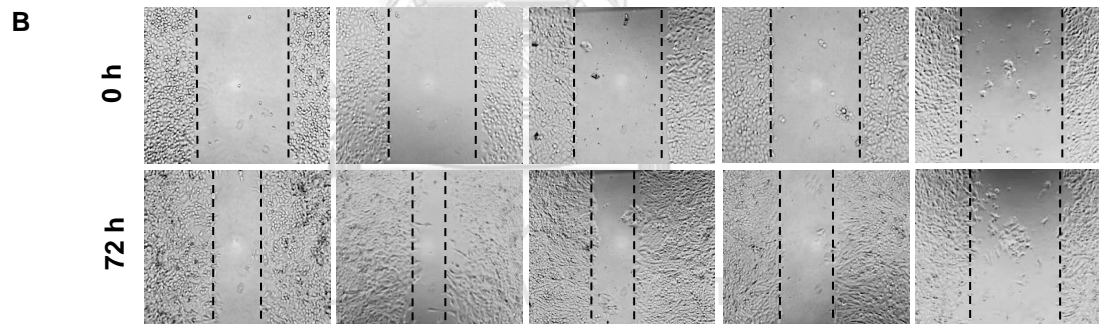
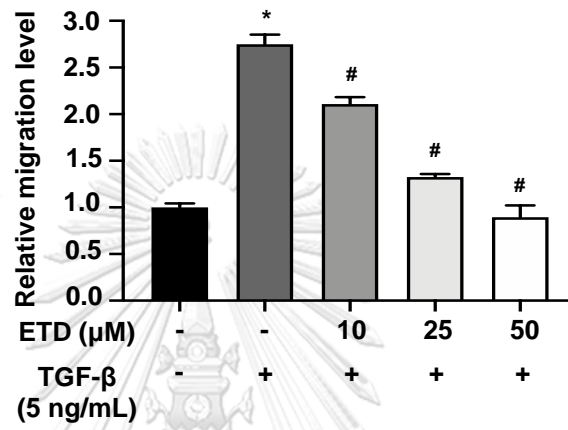
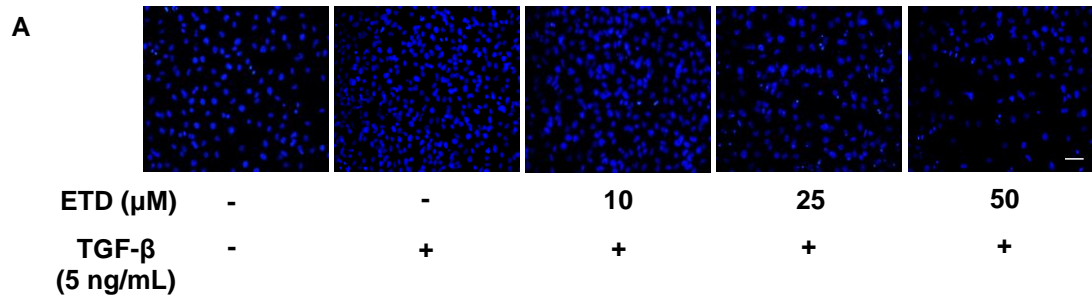


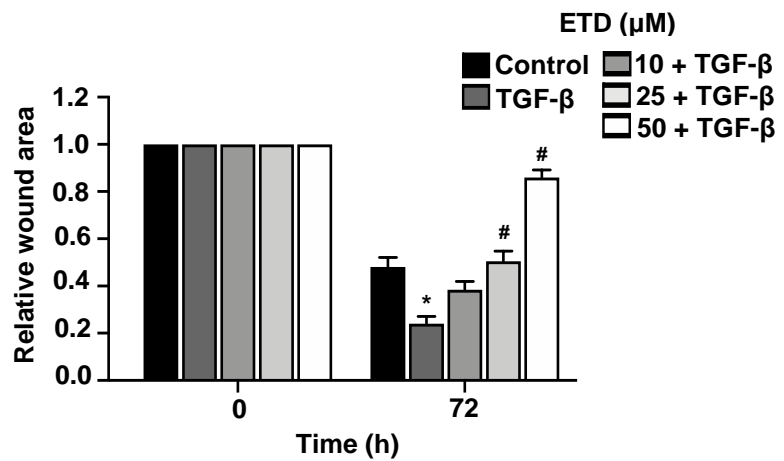
Figure 13 Erianthridin inhibits an anchorage-independent growth of human non-small cell lung cancer cells. Anchorage-independent growth assay were conducted by seeding cells onto 24-well coated with 0.5 % agarose. Cells were incubated with erianthridin and allowed for growth for 10 d. The colonies were stained with crystal violet, and the colony size was measured using ImageJ. Each dot plot represented a single colony. All data are presented as mean \pm SEM (n = 3). * $p < 0.05$ vs untreated control group.

4.5 Erianthridin suppresses TGF- β -induced migration and anchorage-independent growth of human non-small cell lung cancer cells

(TGF- β) has been recognized as an important regulator for tumor progression that promote metastatic behaviors including cell migration, cell invasion and anchorage-independent growth through canonical and canonical pathways (32, 71). We investigated whether erianthridin inhibits TGF- β -induced metastatic capability of non-small-cell lung cancer cells. The transwell migration assay demonstrated that TGF- β enhance the migration ability of A549 cells by approximately 2.5-fold compared with control cells. However, pretreatment of cells with erianthridin significantly suppressed TGF- β -induced cell migration (Figure 14A). Consistently, wound healing assay revealed that TGF- β clearly increased A549 cell migration activity after 72 h of incubation. However, cell migration induced by TGF- β was attenuated in the presence of erianthridin, especially 25 and 50 μ m (Figure 14B). Next, we further investigated whether erianthridin was able to suppress TGF- β -induced cell growth under detachment conditions. Figure 14C revealed that TGF- β caused a significant increase the size of colonies formed on soft agar whereas the colony size pretreated with erianthridin was remarkably reduced in a concentration-dependent manner. These results suggest that erianthridin was able to attenuate TGF- β -induced metastatic behaviors in lung cancer cells.



ETD (μM)	-	-	10	25	50
TGF- β (5 ng/mL)	-	+	+	+	+



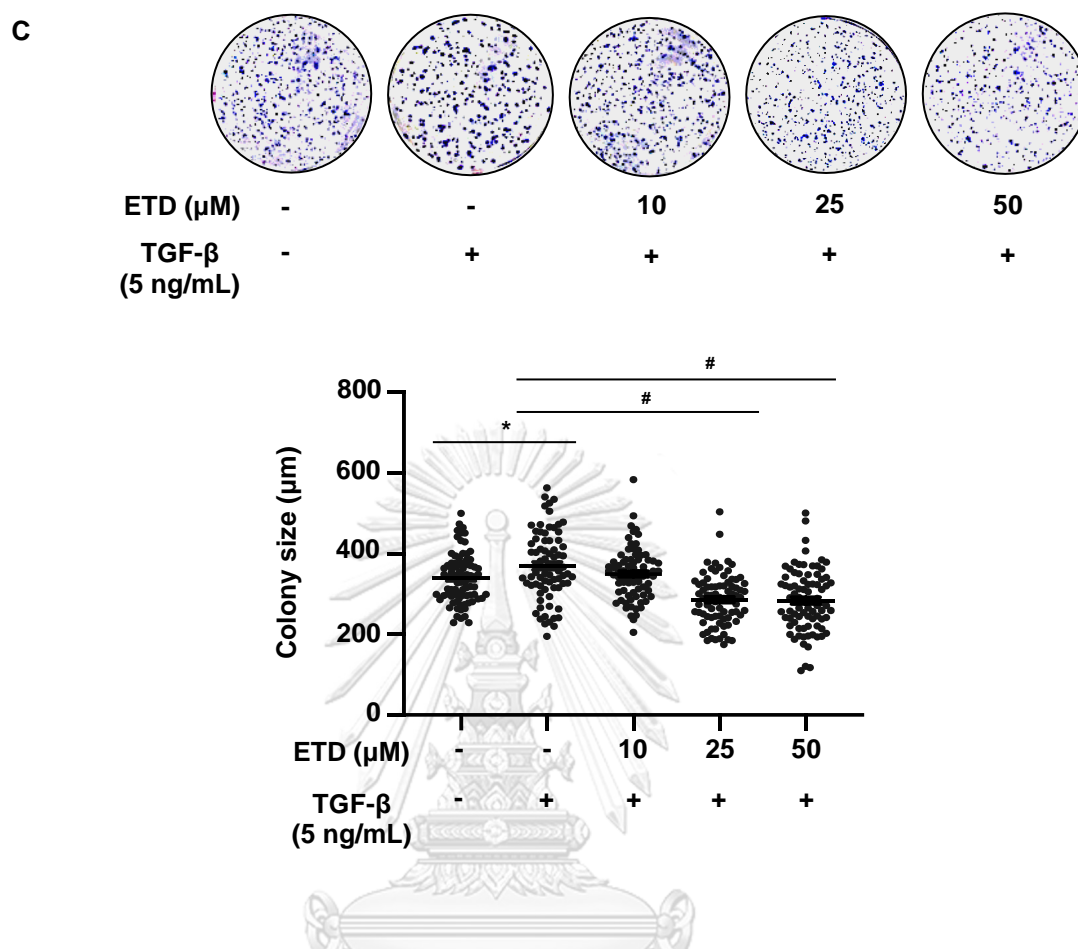
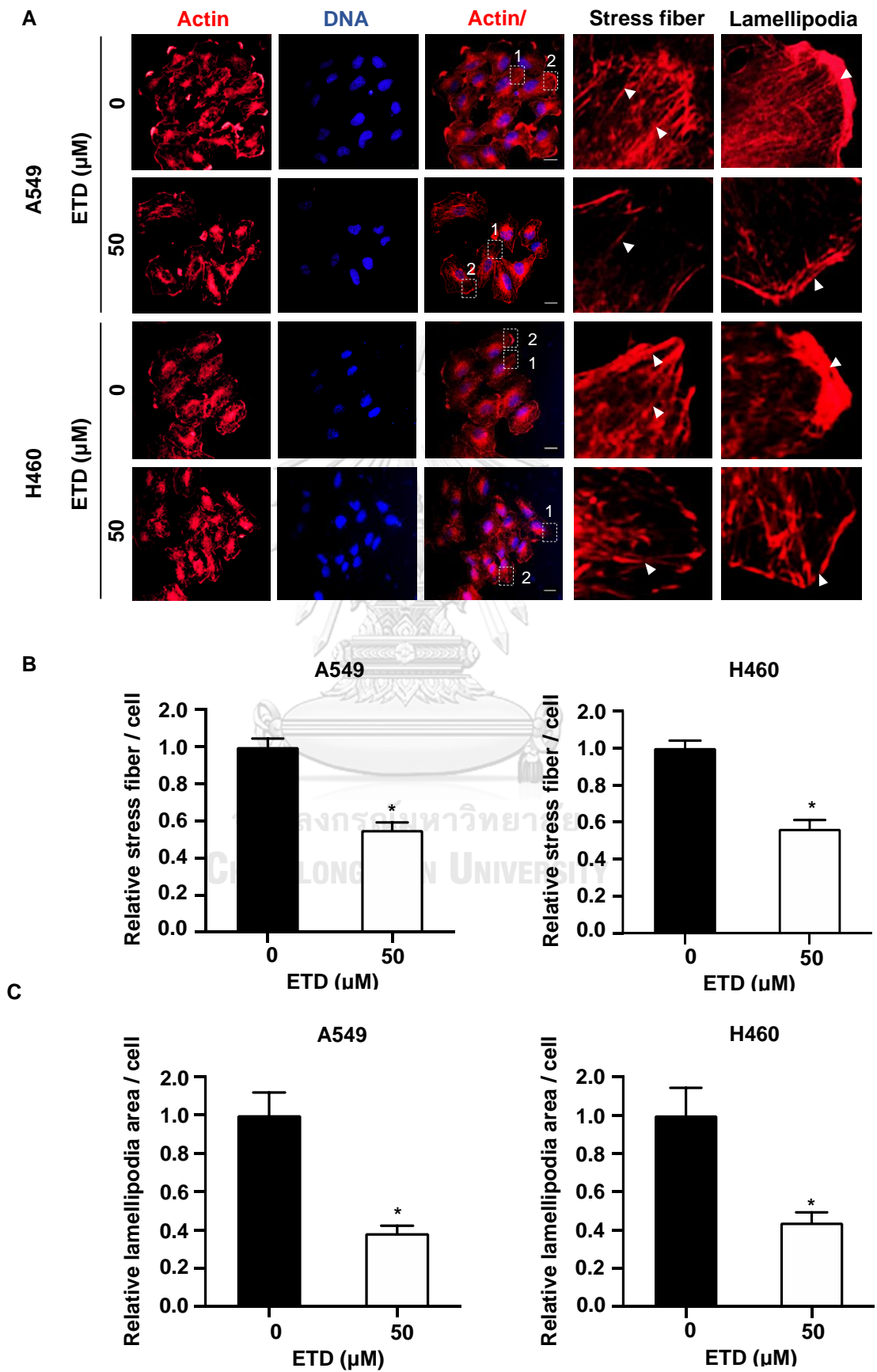


Figure 14 Erianthridin suppresses TGF- β -induced migration and anchorage-independent growth of human non-small-cell lung cancer cells. (A) A549 cells were seeded onto the transwell chamber and incubated with non-toxic dose of erianthridin for 8 h followed by treatment with TGF- β (5 ng/ml) for 12 h. The cells were stained with DAPI and imaged by fluorescence microscopy. The cells on the lower side of transwell were counted and calculated as the relative number of migrated cells of treatment group compared to control group. Scale bar is 10 μm . (B) Monolayer of the cells was scratched with pipette tip to generate wound space and pretreated with 0-50 μM of erianthridin for 8 h followed by treatment with TGF- β . The wound area was photographed under microscope at 0, 72 h. The wound space was quantified as an area at each time point relative to an area at initial time point.

(C) Anchorage-independent growth assay were conducted by seeding cells onto 24-well coated with 0.5 % agarose. Cells were incubated with erianthridin for 8 h followed by treatment with TGF- β and allowed for growing 10 d. The colonies were stained with crystal violet, and the colony size was measured using ImageJ. Each dot plot represented a single colony. All data are presented as mean \pm SEM (n = 3). * p < 0.05 vs untreated control group. # p < 0.05 vs TGF- β treated alone.

4.6 Erianthridin suppresses actin stress fibers and lamellipodia formation through Rac1-dependent pathway

Actin stress fibers are required for cell motility during metastasis by providing the contractile force to push the cell move forward (8). Our results demonstrated that actin stress fibers were clearly present in nontreated cells, but they were markedly reduced after treatment with 50 μ M erianthridin (Figure 15A-B). We also investigated whether erianthridin-attenuating cell motility is involved in the alteration of lamellipodia formation. Immunofluorescence assay revealed that erianthridin effectively disrupted lamellipodial assembly. Quantitative analysis demonstrated that the areas of lamellipodia formation in A549 and H460 cells were notably decreased in the presence of erianthridin (Figure 15C). Since the Rac1 protein plays an important role in actin reorganization (47), the active state of GTP-Rac1 was then examined. Western blot analysis showed that erianthridin strongly suppressed Rac1 activity (Figure 15D), suggesting that erianthridin inhibited these actin dynamics in a Rac1-dependent manner.



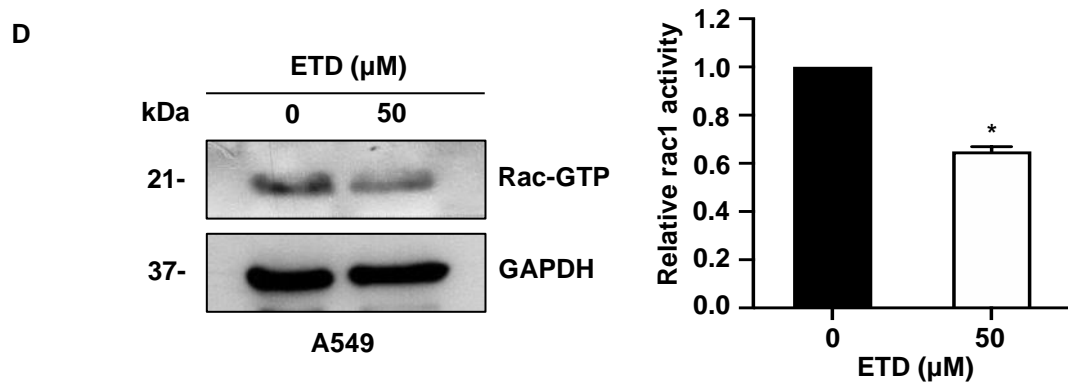


Figure 15 Erianthridin suppresses actin stress fibers and lamellipodia formation through Rac1-dependent pathway. (A) A549 and H460 cells were cultured on cover slips and treated with 50 μM erianthridin for 48 h. Cells were stained with phalloidin (actin, red) and DAPI (blue) and observed by fluorescence microscopy with 200x magnification. The images in the box are enlarged in the right panel. Arrows indicate actin stress fibers and lamellipodia. The scale bar is 20 μm . (B) The number of stress fibers per cell and (C) the area of lamellipodia per cell were analyzed relative to those of the control group using ImageJ. The data are presented as the mean \pm SEM (at least 50 cells/group). * $p < 0.05$ vs untreated control group. (D) Erianthridin inhibits Rac1 activity. A549 cells were treated with 50 μM of erianthridin for 48 h. Rac1 activity was determined by Rac1 activation assay kit. GAPDH was re-probed as a loading control. The intensity was quantified and normalized with loading control by ImageJ. The level of Rac1 activity is plotted as mean \pm SEM ($n = 3$). * $p < 0.05$ vs untreated control group.

4.7 Erianthridin inhibits *MMP-2* and *MMP-9* expressions in non-small cell lung cancer cells

MMP-2 and MMP-9 are known as gelatinase enzymes required for degradation of basement membrane during invasion process. To investigate the effect of erianthridin on these enzyme expressions, *MMP-2* and *MMP-9* expressions were examined by real-time PCR. The results showed that the mRNA levels of *MMP-2* and *MMP-9* were significantly downregulated by erianthridin in a dose-dependent manner (Figure 16A-B). These data suggested that erianthridin suppresses lung cancer cell invasion via reduction of MMPs expression.



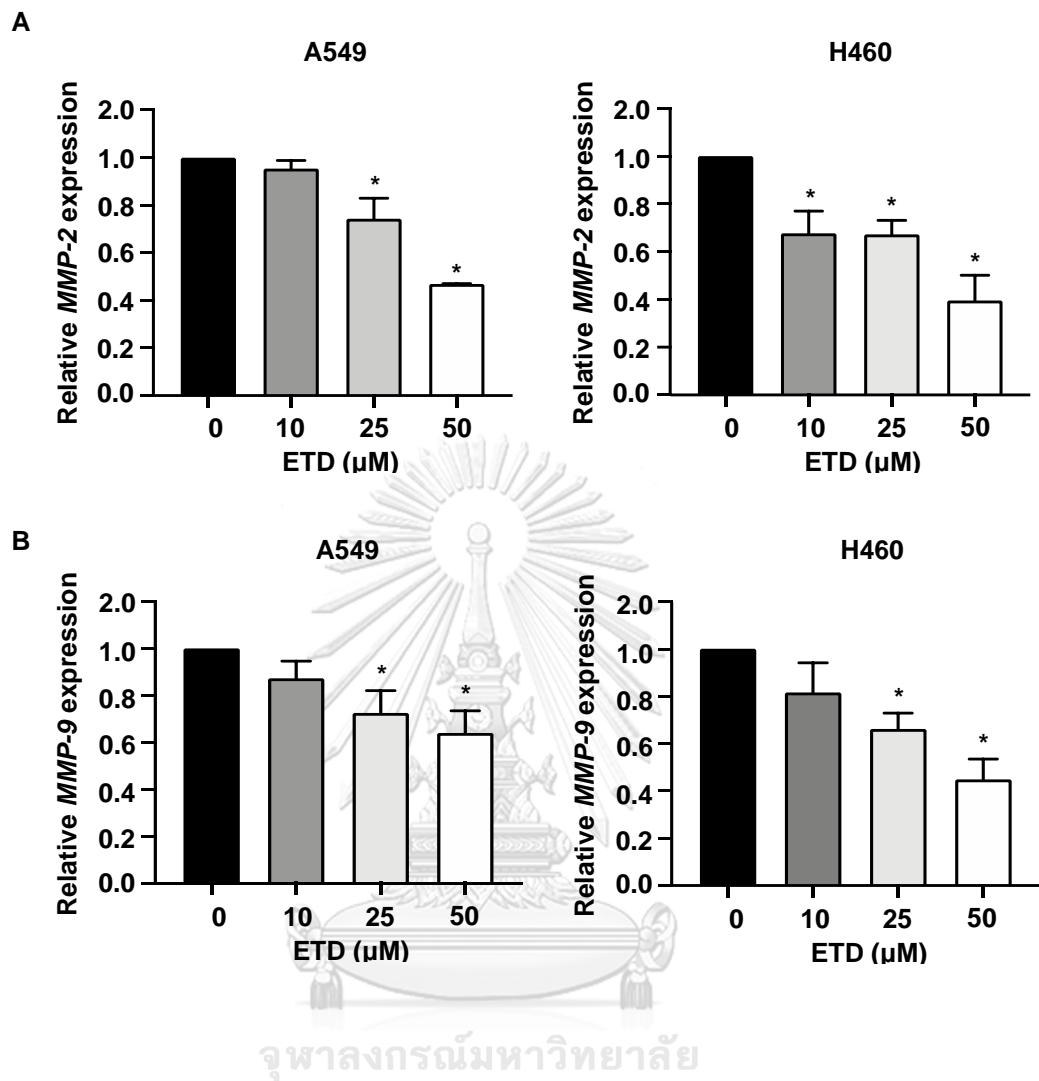
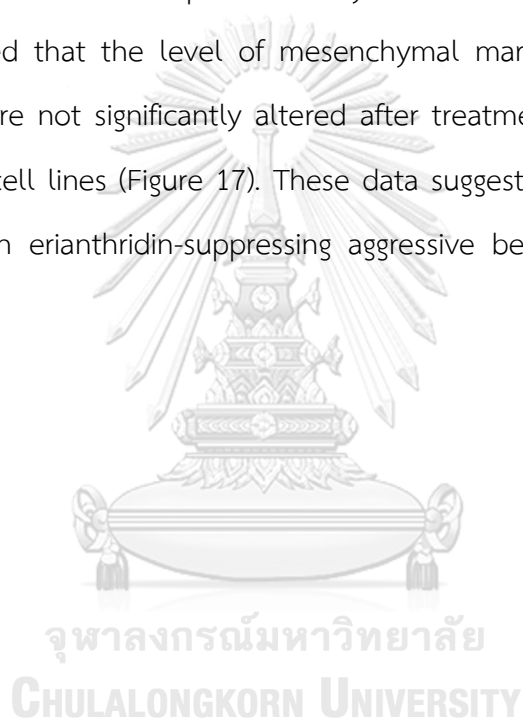


Figure 16 Erianthridin inhibits *MMP-2* and *MMP-9* expression of non-small cell lung cancer. Cells were treated with 0-50 μM erianthridin for 48 h, and (A) *MMP-2* and (B) *MMP-9* mRNA expression was quantified by quantitative real-time PCR. The mRNA expression level of the treatment group was calculated relative to that in the control group. The data are presented as the mean \pm SEM ($n = 3$). * $p < 0.05$ vs untreated control group.

4.8 Erianthridin suppresses cell migration and invasion in an independency of EMT process

Epithelial to mesenchymal transition (EMT) has been reported to enhance the migratory and invasive of cancers by inducing mesenchymal genes. EMT functions as a regulator of mesenchymal phenotypes to promote a change in cell morphology and ECM remodeling (70). To investigate whether erianthridin was able to inhibit EMT, the levels of EMT-marker were performed by western blot analysis. Unexpectedly, the results showed that the level of mesenchymal markers including N-cadherin, Snail and Slug were not significantly altered after treatment of erianthridin in both A549 and H4560 cell lines (Figure 17). These data suggest that EMT mechanism did not participated in erianthridin-suppressing aggressive behaviors of non-small cell lung cancer cells.



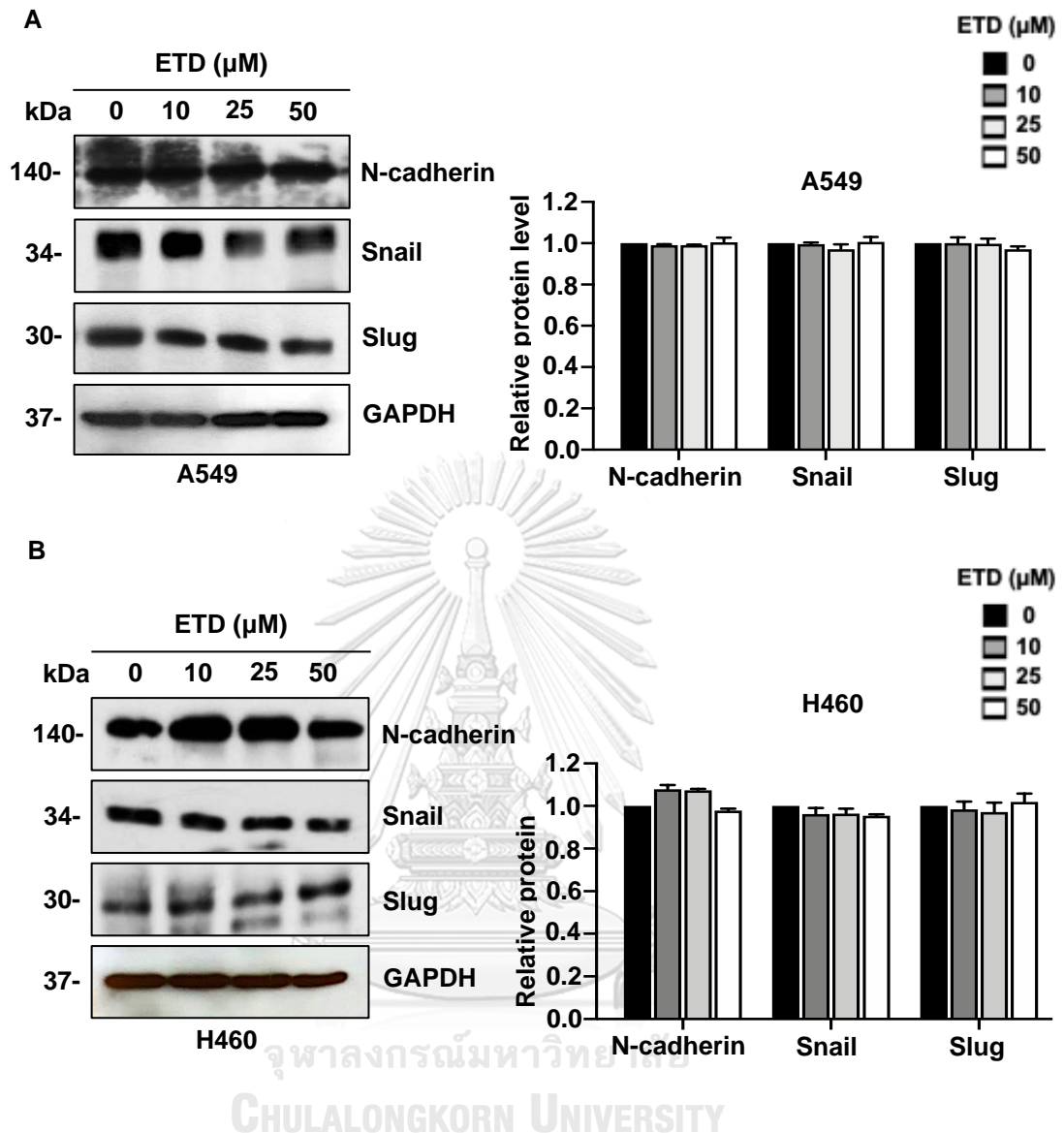


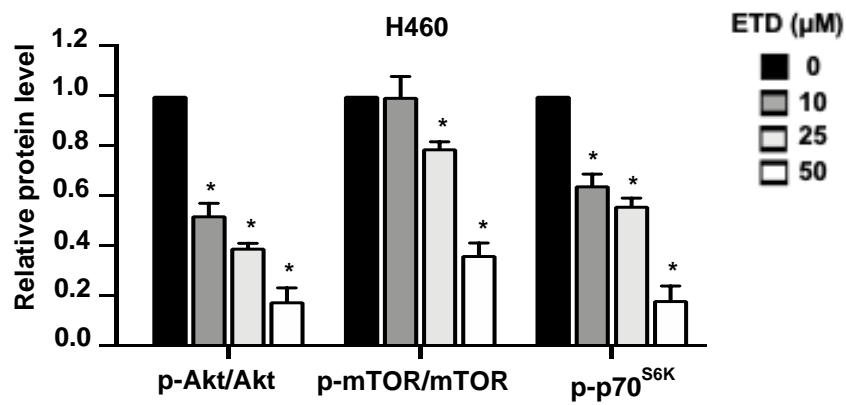
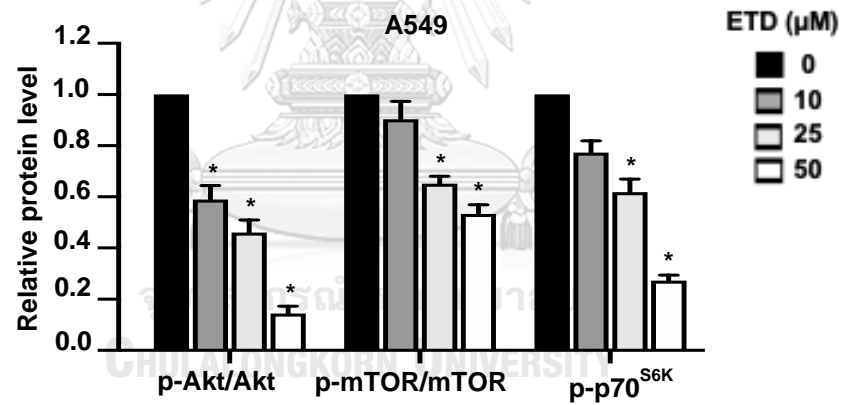
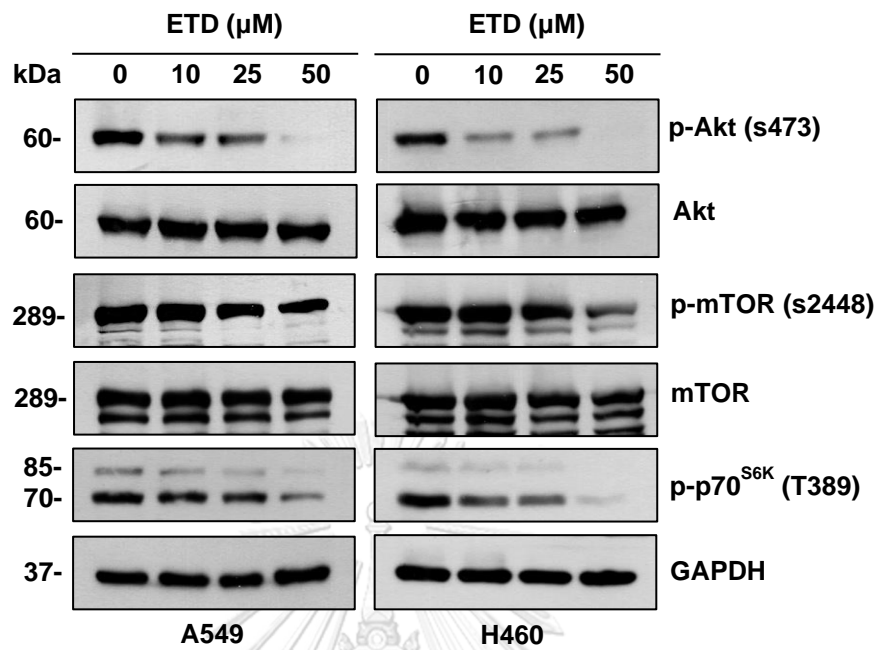
Figure 17 Erianthridin suppresses cell migration and invasion in an independency of EMT process. (A) A549 and (B) H460 cells were treated with non-toxic concentrations of erianthridin (0-50 μM) for 24 h. The protein expression level of N-cadherin, snail and slug were examined by Western blot analysis. GAPDH was reprobred as a loading control. The intensity was qualified and normalized with loading control by ImageJ. The protein expression levels are plotted as mean \pm SEM (n = 3). * p < 0.05 vs untreated control group.

4.9 Eriathridin attenuates Akt/mTOR/p70^{S6K} signaling pathway

The Akt signaling pathway has been reported to control necessary cancer behaviors during metastasis, including cell motility and invasion (63). To explore whether the Akt pathway is involved in erianthridin-mediated suppression of cell migration and invasion, western blot analysis was performed. As seen in Figure 18A, the level of Ser473-phosphorylated Akt, an active state of Akt, was gradually decreased in A549 and H460 cells treated with erianthridin, whereas total Akt was unchanged. Western blot analysis also revealed that erianthridin was able to downregulate the expression levels of p-mTOR (Ser2448) and p-p70^{S6K} (Thr389), members of a downstream signaling axis of Akt that regulates cell motility and invasion, in A549 and H460 cells, suggesting that Akt/mTOR/p70^{S6K} signaling is a possible target by which erianthridin inhibits non-small-cell lung cancer cell migration and invasion.

To confirm whether the Akt pathway and its downstream effectors are required for the inhibitory effects of erianthridin on cell migration and invasion, we knocked down Akt in A549 cells by specific small interfering RNA (siAkt). The results demonstrated that the level of Akt and its active form declined in response to siAkt transfection. In addition, the downstream kinase (p-p70^{S6K}) and p-mTOR were obviously downregulated with Akt phosphorylation (Figure 18B). Furthermore, the reduction in p-p70^{S6K} and p-mTOR became more obvious after treatment with erianthridin in Akt knockdown (A549/siAkt) cells. These data supported our hypothesis that the Akt/mTOR/p70^{S6K} pathway participates in the erianthridin-induced attenuation of cell migration and invasion

A



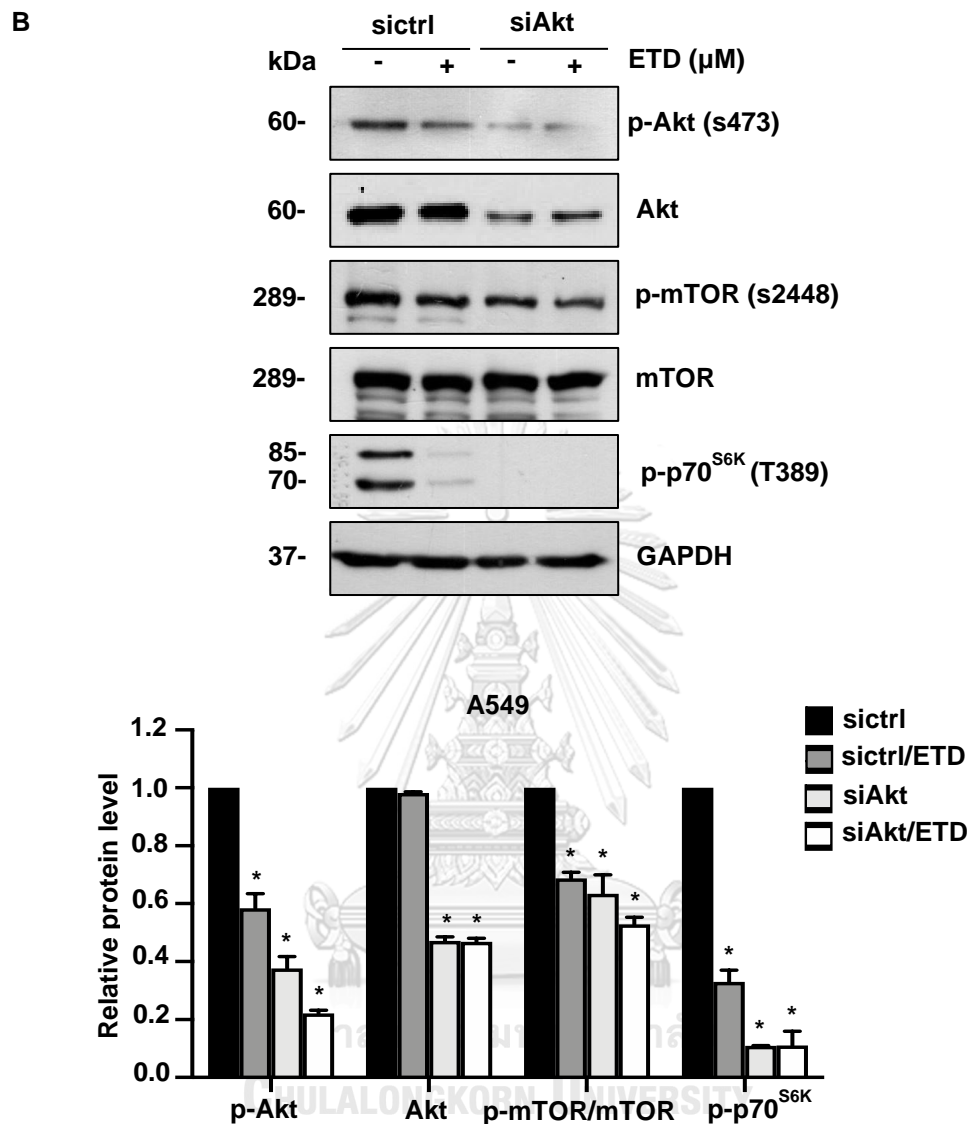


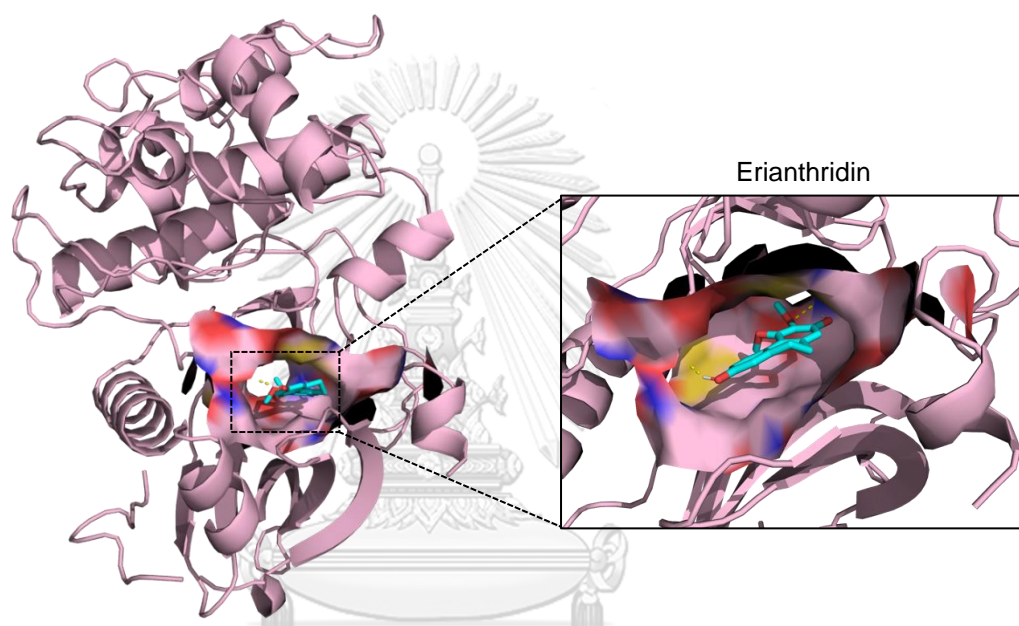
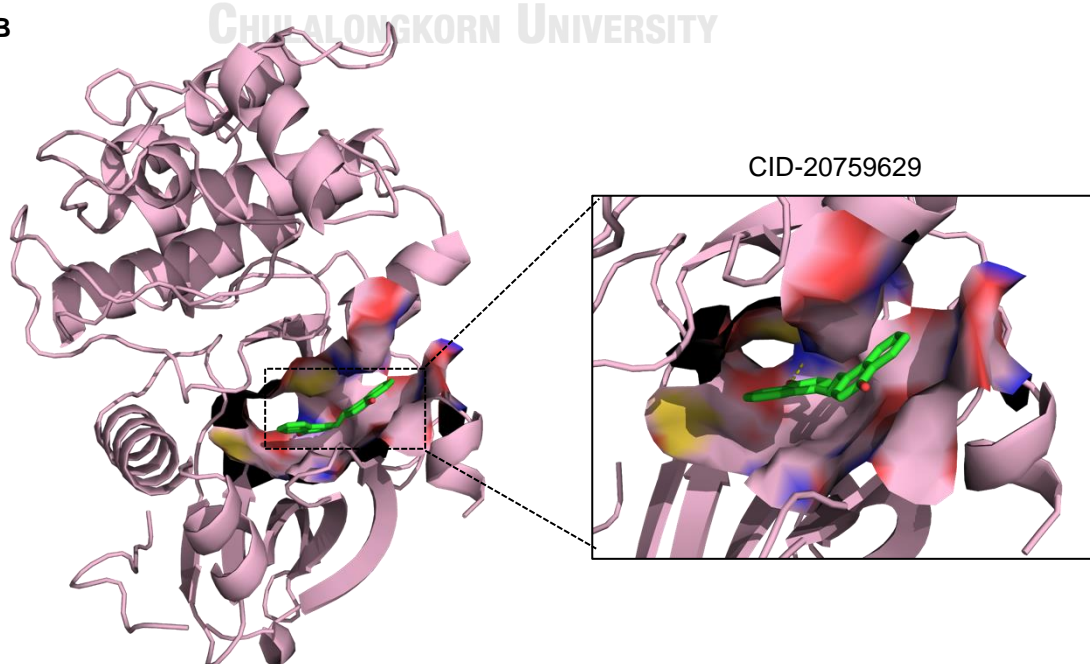
Figure 18 Erianthridin inhibits cell migration and invasion via an Akt/mTOR/p70^{S6K}-dependent mechanism. (A) A549 and H460 cells were treated with nontoxic concentrations of erianthridin for 24 h. The protein expression levels of p-Akt, Akt, p-mTOR, mTOR and p-p70^{S6K} were examined by Western blot analysis. GAPDH was used as a loading control. The intensity was qualified and normalized to that of the loading control with ImageJ. The protein expression levels are displayed as the mean \pm SEM (n = 3). * p < 0.05 vs untreated control group. (B) A549 cells were transfected

with siRNA against Akt (siAkt) or si-mismatch control siRNA (siCtrl). After transfection for 18 h, cells were incubated with 50 μ M erianthridin for 24 h and examined by western blot analysis. GAPDH was used as a loading control. The intensity was qualified and normalized to that of the loading control with ImageJ. The protein expression levels are shown as the mean \pm SEM (n = 3). * p < 0.05 vs untreated A549/siCtrl cells

4.10 Eriathridin possible binds to Akt and inhibits Akt activity

To further investigated whether a decrease in Akt activity might be a result of direct interaction between erianthridin and Akt, *in silico* molecular docking was performed. The results demonstrated that erianthridin binds to the ATP binding site in the protein kinase domain of Akt (Figure 19A). The key interactions stabilizing the complex are hydrogen bonding and van der Waals interactions (Figure 19C). The methoxy and phenol groups of erianthridin can form hydrogen bonds with the amide backbone of Ala230 (1.82 Å), which is a backbone amide in the kinase hinge, and the carboxylic acid side chain of Asp292 (1.93 Å), respectively. Other amino acids forming van der Waals interactions are Leu156, Val164, Ala177, Lys179, Thr211, Met227, Glu228, Tyr229, Met281, Thr291, and Phe438. The methoxy group is oriented towards the gatekeeper Met227. We also compared the binding of erianthridin with CID-20759629, reported ATP competitive inhibitor of AKT1 (72). As shown in Figure 19B, CID-20759629 also interacts with Akt at ATP binding site. CID-20759629 forms only one hydrogen bond between carbonyl functional group and amide backbone of Ala230 (2.89 Å). For Van der Waals interaction, CID-20759629 interacts with almost the same amino acids as erianthridin except Lys179, Met281, Thr291, and Phe438 and has additional interaction with Gly157, Lys158, Glu234, Phe237, Asp439 and Phe442 (Figure 19D). Based on these interactions, the free binding energy between erianthridin and Akt is -8.85 kcal/mol which is higher than CID-20759629 (-11.97

kcal/mol) due to higher number of interacted amino acid residues of CID-20759629. However, the ligand efficiency (LE) calculated by ΔG /number of heavy atoms is not much different. The LE values of erianthridin and CID-20759629 are -0.44 and -0.50, respectively. These data indicate that erianthridin has a potential interaction with Akt and may interfere with Akt phosphorylation.

A**B**

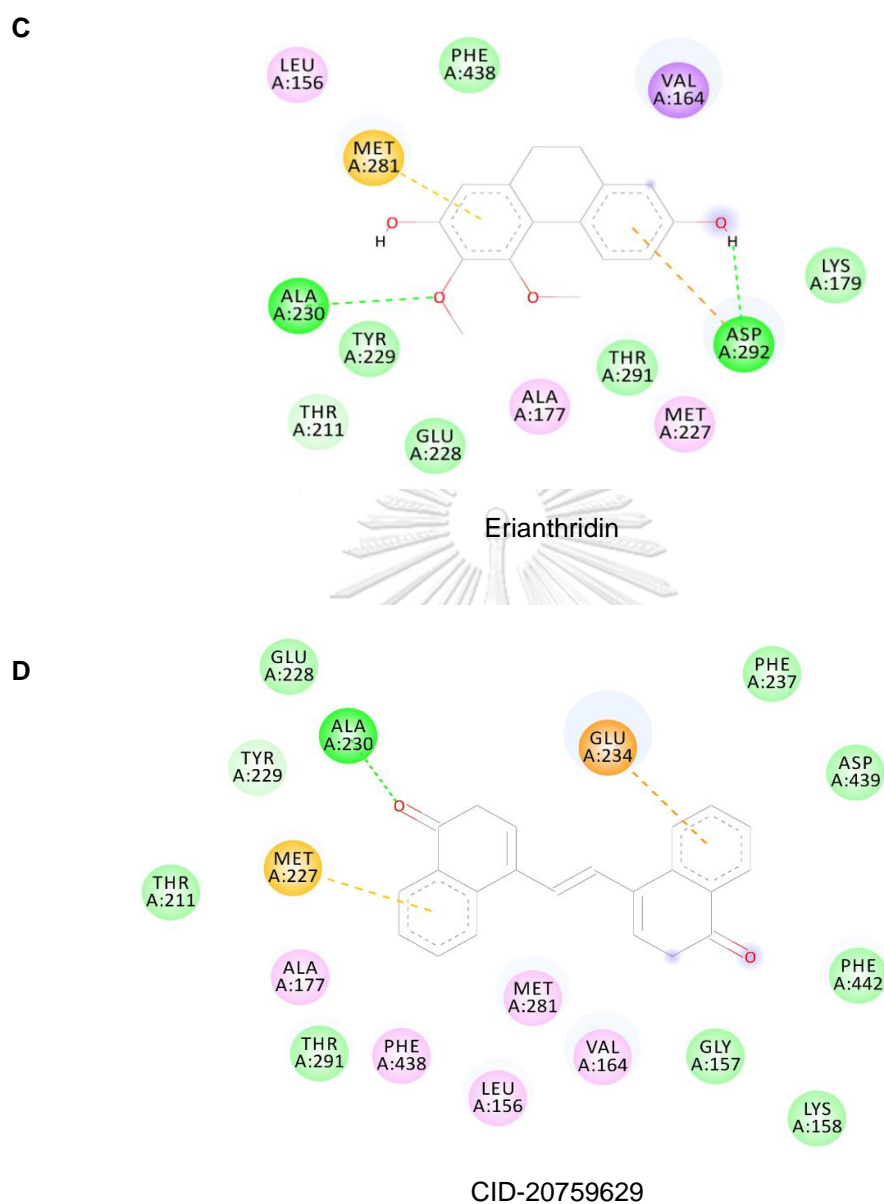


Figure 19 Erianthridin directly binds to Akt. (A), (B) Molecular docking analysis of erianthridin and CID-20759629 with Akt was performed. (C), (D) A schematic diagram of the interacting residues of erianthridin and CID-20759629 with Akt is shown. Hydrogen bonds are displayed in green. The van der Waals interactions are shown in light green and pink. The anion- π and sulfur- π interactions are shown in orange and yellow, respectively.

CHAPTER V

DISCUSSION

Lung cancer is one of the most serious malignancies worldwide due to its rapid metastasis (1). Cell migration and invasion are recognized as critical steps in cancer metastasis, and the inhibition of these aggressive behaviors is of interest as a promising therapeutic approach. Previous studies have reported that phenolic compounds from *Dendrobium* spp. of Thai orchids exhibit antimetastatic activity *via* different molecular mechanisms (16, 17). In the present study, we first demonstrated the potent effect of erianthridin, a phenanthrene derivative isolated from Thai orchids, on suppressing lung cancer metastasis *in vitro* model. Furthermore, the underlying mechanisms are involved regulation of actin cytoskeleton rearrangement and expression *via* the Akt/mTOR/p70^{S6K} signaling pathway.

The migration and invasion of cancer cells are hallmarks of malignancy, enabling cancer cell dissemination to distant organs (4). It has been reported that reorganization of actin filaments is required for cancer cell migration and invasion (7, 8). Dynamic changes in the actin cytoskeleton promote the formation of discrete structures in cancer cells, including lamellipodia and stress fibers, which are essential for directional movement (8, 73). Several studies have demonstrated that disruption of actin structures is able to attenuate migration and invasion abilities in various cancer cell lines (74-76), which is in agreement with our finding that the formation of stress fibers and lamellipodia was obviously disrupted in erianthridin-treated lung cancer cells and consequently resulted in decreased cell motility and invasion. Accumulating studies have revealed that Rac1, a member of the Rho family of small GTPases, participates in the organization of actin filaments and remodeling of the plasma membrane (77). The GTP binding protein Rac1, in its active form, activates the Arp2/3 complex by binding with the SCAR/WAVE regulatory complex, which

promotes the elongation of actin at the leading edge of motile cells (78). Rac1 also functions as a direct regulator of actin stress fiber formation (79). Overactivation of Rac1 has been found in various human cancers, including non-small-cell lung cancer (80). The downregulation of Rac1 was shown to reduce the number of stress fibers and attenuate cancer cell migration and metastasis (81, 82). In agreement with our findings, the disruption of actin-based structures, including stress fibers and lamellipodia, is known to be related to a decrease in the active form of Rac1 in response to erianthridin treatment.

Apart from alteration of actin structures, a degradation of extracellular matrix is required for cell invasion during metastasis. MMP-2 and MMP-9 have a major role in degradation of type IV collagen which is rich in ECM and basement membrane (83). Inhibition of MMP-2 and MMP-9 expression is one of the effective strategies to prevent cancer metastasis. These data are agreement in our finding that anti-invasive of erianthridin resulted from inhibition of *MMP-2* and *MMP-9* expressions in lung cancer cells. It has been reported that the MMPs expression and activity are associated with dynamic change in actin cytoskeleton (84). According to previous study, it has demonstrated that Rac1 significantly increased *MMP-2* and *MMP-9* expressions, conversely, knockdown Rac1 by shRNA show significant reduction of their expressions (85). These data suggest that erianthridin-downregulating *MMP-2* and *MMP-9* expressions may relate to a decrease in Rac1 activity. However, there are several signaling pathway that play an important role in the controlling of *MMP-2* and *MMP-9* expressions including PI3K/Akt signaling pathway (86).

It is well known that PI3K/Akt signaling plays a dominant role in governing cancer cell migration and invasion. The activation of Akt participates in the reorganization of the actin cytoskeleton and mediates contraction of the cellular body through several downstream signaling pathways (87). mTORC1, a downstream

serine threonine kinase effector, was actively phosphorylated at Ser2448 by PI3K/Akt (88). Loss of mTORC1 activity as a consequence of Akt inhibition contributed to a disruption of F-actin organization, including in lamellipodia and filopodia formation, at the leading edge of cancer cells (89). In addition, p70^{S6K} is reported to be a downstream target of the PI3K/Akt/mTORC1 axis (63). p70^{S6K} phosphorylated at Thr389 potentially induces Rac1-mediated lamellipodia formation (12, 13, 87). Inhibition of Akt/mTORC1/p70^{S6K} signaling resulted in an alteration of actin reorganization in favor of impeding cell motility (89), suggesting an intriguing approach for attenuating cancer metastasis. Our findings also demonstrate that erianthridin significantly decreased Akt phosphorylation and activation of its downstream molecules mTOR and p70^{S6K}, leading to the suppression of lung cancer cell migration. Furthermore, several studies have documented that activation of the PI3K/Akt/mTOR/p70^{S6K} signaling pathway triggers the expression of proteolytic enzymes facilitating cancer invasion, including *MMP-2* and *MMP-9* (14) (90), and in particular, p70^{S6K} is an important transcription factor responsible for *MMP-9* synthesis (90). Based on this evidence, the reduction in *MMP-2* and *MMP-9* expression induced by erianthridin in lung cancer cells is a consequence of inactivation of Akt and its downstream effectors.

By considering to the molecular structure of erianthridin, we further revealed how erianthridin has an inhibitory effect on Akt and whether there (KD) is an interaction among them. Akt consists of pleckstrin homology (PH), central kinase domain, and regulatory domain, and its activity is regulated by phosphorylation and dephosphorylation processes in an Akt conformation-dependent manner. ATP-binding site is located at the central kinase domain of Akt, and the interaction of ATP with its pocket site can stabilize active conformation of kinase, resulting in a decrease rate of Akt dephosphorylation (91). To date, the most of Akt inhibitors are small

molecule ATP-competitive inhibitors that have been proven to potently inhibit Akt activity in *in vitro* and *in vivo* models. Occupancy of the pocket by ATP-competitive inhibitor induces the conformation change of Akt leading to destabilization of phosphorylated Akt (91, 92). Our study also demonstrated that erianthridin could be an effective ATP-competitive inhibitor via direct interaction with several amino acid residues in ATP-binding site. The interacting residues of erianthridin was shown to overlap with the reported ATP competitive Akt inhibitors such as CID-20759629, A-674563 and WFE (72, 93, 94).

EMT is one of the crucial processes driving cancer metastasis. It involves genotypic and phenotypic changes of cells from an epithelial-like morphology to cells with loose cell-cell adhesion and a mesenchymal-like morphology (95). Epithelial cells undergoing EMT decrease the expression of cell adhesion molecules, elevate the expression of mesenchymal markers and rearrange their cytoskeletons (95, 96). TGF- β , a multifunctional cytokine involved in many tumor cell functions, is a key modulator of the EMT mechanism (97). The binding of TGF- β to its receptor initiates SMAD phosphorylation and activates downstream cascades in the canonical pathway (98). TGF- β mediates EMT-associated transcription factors (TFs), including those of the Snail and the Slug families, and repressors of the E-cadherin promoter through SMAD signaling, which suppresses the expression of cell adhesion molecules (30). In this study, we found that erianthridin was able to suppress TGF- β -induced metastatic phenotypes in A549 cells; however, erianthridin had no effect on Snail and Slug, a direct transcriptional repressor of E-cadherin, and N-cadherin expression. Since TGF- β -mediated EMT occurs through canonical *and* noncanonical pathways (71), these data suggest that erianthridin diminishes TGF- β -induced metastatic phenotypes independent of canonical mechanisms. In addition, PI3K/Akt and the Rho GTPase family were reported to participate in a noncanonical pathway contributing

to TGF- β -induced EMT (71, 99), suggesting that the inhibitory effect of erianthridin on TGF- β -enhanced cell migration is caused by erianthridin-induced suppression of Akt signaling and Rac1.

In conclusion, this study demonstrated that erianthridin attenuates lung cancer cell metastasis *in vitro* studies. Erianthridin exhibits an inhibitory effect on lung cancer cell migration and invasion *via* the regulation of actin reorganization and MMPs expression, which was induced through Akt and its downstream effectors mTOR and p70^{S6K} (Figure 20). This study suggests that the novel pharmacological activity of erianthridin warrants further research and development of this compound for ultimate use against non-small-cell lung cancer metastasis.

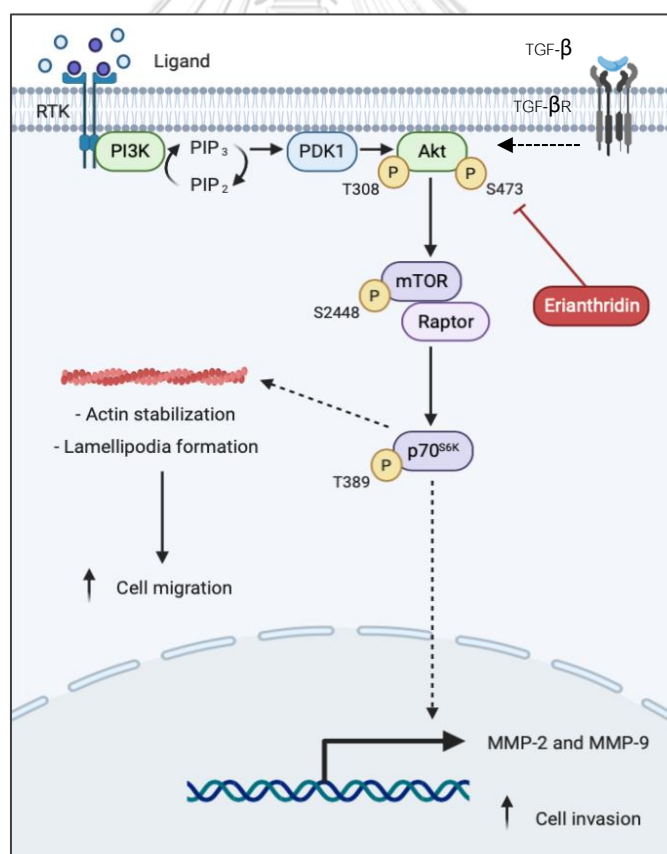


Figure 20 A Scheme diagram of this study. Erianthridin suppresses lung cancer cell migration and invasion through inhibition of Akt/mTOR/p-p70^{S6K} signaling pathway.

REFERENCES

1. Bray F, Ferlay J, Soerjomataram I, Siegel RL, Torre LA, Jemal A. Global cancer statistics 2018: GLOBOCAN estimates of incidence and mortality worldwide for 36 cancers in 185 countries. *CA Cancer J Clin.* 2018;68(6):394-424.
2. Subotic D, Van Schil P, Grigoriu B. Optimising treatment for post-operative lung cancer recurrence. *Eur Respir J.* 2016;47(2):374-8.
3. Yang L, Wang Z, Xu L. Simultaneous determination of phenols (bibenzyl, phenanthrene, and fluorenone) in *Dendrobium* species by high-performance liquid chromatography with diode array detection. *J Chromatogr A.* 2006;1104(1-2):230-7.
4. Lambert AW, Pattabiraman DR, Weinberg RA. Emerging biological principles of metastasis. *Cell.* 2017;168(4):670-91.
5. Lintz M, Munoz A, Reinhart-King CA. The Mechanics of Single Cell and Collective Migration of Tumor Cells. *J Biomech Eng.* 2017;139(2).
6. Yilmaz M, Christofori G. Mechanisms of motility in metastasizing cells. *Mol Cancer Res.* 2010;8(5):629-42.
7. Yamaguchi H, Condeelis J. Regulation of the actin cytoskeleton in cancer cell migration and invasion. *Biochim Biophys Acta.* 2007;1773(5):642-52.
8. Tojkander S, Gateva G, Lappalainen P. Actin stress fibers--assembly, dynamics and biological roles. *J Cell Sci.* 2012;125(8):1855-64.
9. Lawson CD, Ridley AJ. Rho GTPase signaling complexes in cell migration and invasion. *J Cell Biol.* 2018;217(2):447-57.
10. Webb AH, Gao BT, Goldsmith ZK, Irvine AS, Saleh N, Lee RP, et al. Inhibition of MMP-2 and MMP-9 decreases cellular migration, and angiogenesis in in vitro models of retinoblastoma. *BMC Cancer.* 2017;17(1):434-44.

11. Qian Y, Corum L, Meng Q, Blenis J, Zheng JZ, Shi X, et al. PI3K induced actin filament remodeling through Akt and p70S6K1: implication of essential role in cell migration. *Am J Physiol Cell Physiol*. 2004;286(1):C153-63.
12. Ip CK, Wong AS. p70 S6 kinase and actin dynamics: A perspective. *Spermatogenesis*. 2012;2(1):44-52.
13. Ip CK, Cheung AN, Ngan HY, Wong AS. p70 S6 kinase in the control of actin cytoskeleton dynamics and directed migration of ovarian cancer cells. *Oncogene*. 2011;30(21):2420-32.
14. Tan W, Zhu S, Cao J, Zhang L, Li W, Liu K, et al. Inhibition of MMP-2 expression enhances the antitumor effect of sorafenib in hepatocellular carcinoma by suppressing the PI3K/AKT/mTOR Pathway. *Oncol Res*. 2017;25(9):1543-53.
15. Unahabhokha T, Chanvorachote P, Sritularak B, Kitsongsermthon J, Pongrakhananon V. Gigantol inhibits epithelial to mesenchymal process in human lung cancer cells. *Evid Based Complement Alternat Med*. 2016;2016:4561674.
16. Kowitdamrong A, Chanvorachote P, Sritularak B, Pongrakhananon V. Moscatilin inhibits lung cancer cell motility and invasion via suppression of endogenous reactive oxygen species. *Biomed Res Int*. 2013;2013:765894.
17. Treesuwan S, Sritularak B, Chanvorachote P, Pongrakhananon V. Cyprisedin diminishes an epithelial-to-mesenchymal transition in non-small cell lung cancer cells through suppression of Akt/GSK-3beta signalling. *Sci Rep*. 2018;8(1):8009.
18. Lin CW, Hwang TL, Chen FA, Huang CH, Hung HY, Wu TS. Chemical constituents of the rhizomes of *Bletilla formosana* and their potential anti-inflammatory activity. *J Nat Prod*. 2016;79(8):1911-21.
19. Rendon-Vallejo P, Hernandez-Abreu O, Vergara-Galicia J, Millan-Pacheco C, Mejia A, Ibarra-Barajas M, et al. Ex vivo study of the vasorelaxant activity induced by phenanthrene derivatives isolated from *Maxillaria densa*. *J Nat Prod*. 2012;75(12):2241-5.

20. de Groot PM, Wu CC, Carter BW, Munden RFJTLcr. The epidemiology of lung cancer. 2018;7(3):220.
21. Quoix E. Advanced non-small cell lung cancer in elderly patients. *Breathe*. 2012;9(1):26-34.
22. Gridelli C, Aapro M, Ardizzoni A, Balducci L, De Marinis F, Kelly K, et al. Treatment of advanced non-small-cell lung cancer in the elderly: results of an international expert panel. *J Clin Oncol*. 2005;23(13):3125-37.
23. Kalluri R, Weinberg RA. The basics of epithelial-mesenchymal transition. *J Clin Invest*. 2009;119(6):1420-8.
24. Petrova YI, Schecterson L, Gumbiner BM. Roles for E-cadherin cell surface regulation in cancer. *Mol Biol Cell*. 2016;27(21):3233-44.
25. Song Y, Ye M, Zhou J, Wang ZW, Zhu X. Restoring E-cadherin Expression by Natural Compounds for Anticancer Therapies in Genital and Urinary Cancers. *Mol Ther Oncolytics*. 2019;14:130-8.
26. Yu W, Yang L, Li T, Zhang Y. Cadherin signaling in cancer: Its functions and role as a therapeutic target. *Front Oncol*. 2019;9:989.
27. Liu CY LH, Tang MJ, Wang YK. Vimentin contributes to epithelial-mesenchymal transition cancer cell mechanics by mediating cytoskeletal organization and focal adhesion maturation. *Oncotarget*. 2015;6(18):15966.
28. Liu F, Gu LN, Shan BE, Geng CZ, Sang MX. Biomarkers for EMT and MET in breast cancer: An update. *Oncol Lett*. 2016;12(6):4869-76.
29. Zeisberg M, Neilson EG. Biomarkers for epithelial-mesenchymal transitions. *J Clin Invest*. 2009;119(6):1429-37.
30. Morandi A, Taddei ML, Chiarugi P, Giannoni E. Targeting the metabolic reprogramming that controls epithelial-to-mesenchymal transition in aggressive tumors. *Front Oncol*. 2017;7:40.

31. Yeo CD, Kang N, Choi SY, Kim BN, Park CK, Kim JW, et al. The role of hypoxia on the acquisition of epithelial-mesenchymal transition and cancer stemness: a possible link to epigenetic regulation. *Korean J Intern Med.* 2017;32(4):589-99.
32. Wendt MK, Allington TM, Schiemann WP. Mechanisms of the epithelial-mesenchymal transition by TGF-beta. *Future Oncol.* 2009;5(8):1145-68.
33. Lo UG, Lee CF, Lee MS, Hsieh JT. The role and mechanism of epithelial-to-mesenchymal transition in prostate cancer progression. *Int J Mol Sci.* 2017;18(10):2079.
34. Miyoshi A, Kitajima Y, Sumi K, Sato K, Hagiwara A, Koga Y, et al. Snail and SIP1 increase cancer invasion by upregulating MMP family in hepatocellular carcinoma cells. *Br J Cancer.* 2004;90(6):1265-73.
35. Xu W, Yang Z, Lu N. A new role for the PI3K/Akt signaling pathway in the epithelial-mesenchymal transition. *Cell Adh Migr.* 2015;9(4):317-24.
36. Wong TS, Gao W, Chan JY. Transcription regulation of E-cadherin by zinc finger E-box binding homeobox proteins in solid tumors. *Biomed Res Int.* 2014;2014:921564.
37. Gregory PA, Bracken CP, Smith E, Bert AG, Wright JA, Roslan S, et al. An autocrine TGF-beta/ZEB/miR-200 signaling network regulates establishment and maintenance of epithelial-mesenchymal transition. *Mol Biol Cell.* 2011;22(10):1686-98.
38. Zhang W, Shi X, Peng Y, Wu M, Zhang P, Xie R, et al. HIF-1alpha promotes epithelial-mesenchymal transition and metastasis through direct regulation of ZEB1 in colorectal cancer. *PLoS One.* 2015;10(6):e0129603.
39. Izdebska M, Zielinska W, Grzanka D, Gagat M. The Role of actin dynamics and actin-binding proteins expression in epithelial-to-mesenchymal transition and its association with cancer progression and evaluation of possible therapeutic targets. *Biomed Res Int.* 2018;2018:4578373.

40. Yang J, Weinberg RA. Epithelial-mesenchymal transition: at the crossroads of development and tumor metastasis. *Dev Cell*. 2008;14(6):818-29.
41. Arjonen A, Kaukonen R, Ivaska J. Filopodia and adhesion in cancer cell motility. *Cell Adh Migr*. 2011;5(5):421-30.
42. Xue F, Janzen DM, Knecht DA. Contribution of filopodia to cell migration: A mechanical link between protrusion and contraction. *Int J Cell Biol*. 2010;2010:507821.
43. Newell-Litwa KA, Horwitz R, Lamers ML. Non-muscle myosin II in disease: mechanisms and therapeutic opportunities. *Dis Model Mech*. 2015;8(12):1495-515.
44. Innocenti M. New insights into the formation and the function of lamellipodia and ruffles in mesenchymal cell migration. *Cell Adh Migr*. 2018;12(5):401-16.
45. Mattila PK, Lappalainen P. Filopodia: molecular architecture and cellular functions. *Nat Rev Mol Cell Biol*. 2008;9(6):446-54.
46. Cardama GA, Gonzalez N, Maggio J, Menna PL, Gomez DE. Rho GTPases as therapeutic targets in cancer (Review). *Int J Oncol*. 2017;51(4):1025-34.
47. Ridley AJ. Rho GTPase signalling in cell migration. *Curr Opin Cell Biol*. 2015;36:103-12.
48. Suetsugu S, TT. Regulation of cortical actin networks in cell migration. *International review of cytology*. 2003;229:245-86.
49. Smith LG, Li R. Actin Polymerization: Riding the Wave. *Current Biology*. 2004;14(3):R109-R11.
50. ohatgi R HH, Kirschner MW. . Mechanism of N-WASP activation by CDC42 and phosphatidylinositol 4, 5-bisphosphate. *Journal of Cell Biology*.150(6):1299-310.
51. Bosman FT, Stamenkovic I. Functional structure and composition of the extracellular matrix. *J Pathol*. 2003;200(4):423-8.

52. Pittayapruek P, Meephansan J, Prapapan O, Komine M, Ohtsuki M. Role of matrix metalloproteinases in photoaging and photocarcinogenesis. *Int J Mol Sci.* 2016;17(6):868.
53. Wang QM, Lv L, Tang Y, Zhang L, Wang LF. MMP-1 is overexpressed in triple-negative breast cancer tissues and the knockdown of MMP-1 expression inhibits tumor cell malignant behaviors in vitro. *Oncol Lett.* 2019;17(2):1732-40.
54. Kudo Y, Iizuka S, Yoshida M, Tsunematsu T, Kondo T, Subarnbhesaj A, et al. Matrix metalloproteinase-13 (MMP-13) directly and indirectly promotes tumor angiogenesis. *J Biol Chem.* 2012;287(46):38716-28.
55. Dong W, Li H, Zhang Y, Yang H, Guo M, Li L, et al. Matrix metalloproteinase 2 promotes cell growth and invasion in colorectal cancer. *Acta Biochim Biophys Sin (Shanghai).* 2011;43(11):840-8.
56. Mehner C HA, Miller E, Ran S, Radisky DC, Radisky ES. Tumor cell-produced matrix metalloproteinase 9 (MMP-9) drives malignant progression and metastasis of basal-like triple negative breast cancer. *Oncotarget.* 2014;5(9):2736.
57. Itoh Y. Membrane-type matrix metalloproteinases: Their functions and regulations. *Matrix Biol.* 2015;44-46:207-23.
58. Paoli P, Giannoni E, Chiarugi P. Anoikis molecular pathways and its role in cancer progression. *Biochim Biophys Acta.* 2013;1833(12):3481-98.
59. Martin SS, Vuori K. Regulation of Bcl-2 proteins during anoikis and amorphosis. *Biochim Biophys Acta.* 2004;1692(2-3):145-57.
60. Jennings S, Pham T, Ireland SK, Ruoslahti E, Biliran H. Bit1 in anoikis resistance and tumor metastasis. *Cancer Lett.* 2013;333(2):147-51.
61. Karimi Roshan M, Soltani A, Soleimani A, Rezaie Kahkhaie K, Afshari AR, Soukhtanloo M. Role of AKT and mTOR signaling pathways in the induction of epithelial-mesenchymal transition (EMT) process. *Biochimie.* 2019;165:229-34.

62. Manning BD, Cantley LC. AKT/PKB signaling: navigating downstream. *Cell*. 2007;129(7):1261-74.
63. Xue G, Hemmings BA. PKB/Akt-dependent regulation of cell motility. *J Natl Cancer Inst*. 2013;105(6):393-404.
64. Pon YL, Zhou HY, Cheung AN, Ngan HY, Wong AS. p70 S6 kinase promotes epithelial to mesenchymal transition through snail induction in ovarian cancer cells. *Cancer Res*. 2008;68(16):6524-32.
65. Cai W YQ, She QB. Loss of 4E-BP1 function induces EMT and promotes cancer cell migration and invasion via cap-dependent translational activation of snail. *Oncotarget*. 2014 5(15):6015.
66. Chen H, Huang Y, Huang J, Lin L, Wei G. Gigantol attenuates the proliferation of human liver cancer HepG2 cells through the PI3K/Akt/NF-kappaB signaling pathway. *Oncol Rep*. 2017;37(2):865-70.
67. Morris GM, Huey R, Lindstrom W, Sanner MF, Belew RK, Goodsell DS, et al. AutoDock4 and AutoDockTools4: Automated docking with selective receptor flexibility. *J Comput Chem*. 2009;30(16):2785-91.
68. Jaikhan P, Boonyarat C, Arunrungvichian K, Taylor P, Vajragupta O. Design and synthesis of nicotinic acetylcholine receptor antagonists and their effect on cognitive impairment. *Chem Biol Drug Des*. 2016;87(1):39-56.
69. De Pascalis C, Etienne-Manneville S. Single and collective cell migration: the mechanics of adhesions. *Mol Biol Cell*. 2017;28(14):1833-46.
70. Pearson GW. Control of Invasion by Epithelial-to-mesenchymal transition programs during metastasis. *J Clin Med*. 2019;8(5):646.
71. Zhang YE. Non-Smad pathways in TGF-beta signaling. *Cell Res*. 2009;19(1):128-39.

72. Rehan M, Bajouh OSJJob. Virtual screening of naphthoquinone analogs for potent inhibitors against the cancer-signaling PI3K/AKT/mTOR pathway. 2019;120(2):1328-39.
73. Olson MF, Sahai E. The actin cytoskeleton in cancer cell motility. Clin Exp Metastasis. 2009;26(4):273-87.
74. Yamada H, Abe T, Li SA, Masuoka Y, Isoda M, Watanabe M, et al. Dynasore, a dynamin inhibitor, suppresses lamellipodia formation and cancer cell invasion by destabilizing actin filaments. Biochem Biophys Res Commun. 2009;390(4):1142-8.
75. Hayashi K, Michiue H, Yamada H, Takata K, Nakayama H, Wei FY, et al. Fluvoxamine, an anti-depressant, inhibits human glioblastoma invasion by disrupting actin polymerization. Sci Rep. 2016;6:23372.
76. Schenk M, Aykut B, Teske C, Giese NA, Weitz J, Welsch T. Salinomycin inhibits growth of pancreatic cancer and cancer cell migration by disruption of actin stress fiber integrity. Cancer Lett. 2015;358(2):161-9.
77. Parri M, Chiarugi P. Rac and Rho GTPases in cancer cell motility control. Cell Commun Signal. 2010;8:23.
78. Chen B, Chou HT, Brautigam CA, Xing W, Yang S, Henry L, et al. Rac1 GTPase activates the WAVE regulatory complex through two distinct binding sites. Elife. 2017;6.
79. Kovac B, Teo JL, Makela TP, Vallenius T. Assembly of non-contractile dorsal stress fibers requires alpha-actinin-1 and Rac1 in migrating and spreading cells. J Cell Sci. 2013;126(Pt 1):263-73.
80. Zhou Y, Liao Q, Han Y, Chen J, Liu Z, Ling H, et al. Rac1 overexpression is correlated with epithelial mesenchymal transition and predicts poor prognosis in non-small cell lung cancer. J Cancer. 2016;7(14):2100-9.

81. Guo F, Debidda M, Yang L, Williams DA, Zheng Y. Genetic deletion of Rac1 GTPase reveals its critical role in actin stress fiber formation and focal adhesion complex assembly. *J Biol Chem*. 2006;281(27):18652-9.
82. Chen QY, Xu LQ, Jiao DM, Yao QH, Wang YY, Hu HZ, et al. Silencing of Rac1 modifies lung cancer cell migration, invasion and actin cytoskeleton rearrangements and enhances chemosensitivity to antitumor drugs. *Int J Mol Med*. 2011;28(5):769-76.
83. Merchant N, Nagaraju GP, Rajitha B, Lammata S, Jella KK, Buchwald ZS, et al. Matrix metalloproteinases: their functional role in lung cancer. *Carcinogenesis*. 2017;38(8):766-80.
84. Bilyug N. Matrix metalloproteinases: an emerging role in regulation of actin microfilament system. *Biomol Concepts*. 2016;7(5-6):321-9.
85. Chen QY, Zheng Y, Jiao DM, Chen FY, Hu HZ, Wu YQ, et al. Curcumin inhibits lung cancer cell migration and invasion through Rac1-dependent signaling pathway. *J Nutr Biochem*. 2014;25(2):177-85.
86. Reuben PM CH. Regulation of matrix metalloproteinase (MMP) gene expression by protein kinases. *Front Biosci*. 2006;11:1199-215.
87. Qian Y CL, Meng Q, Blenis J, Zheng JZ, Shi X, Flynn DC, Jiang BH. PI3K induced actin filament remodeling through Akt and p70S6K1: implication of essential role in cell migration. *American Journal of Physiology-Cell Physiology*. 2004;286(1):C153-C63.
88. Rosner M, Siegel N, Valli A, Fuchs C, Hengstschlager M. mTOR phosphorylated at S2448 binds to raptor and rictor. *Amino Acids*. 2010;38(1):223-8.
89. Jeong YJ, Hwang SK, Magae J, Chang YC. Ascofuranone suppresses invasion and F-actin cytoskeleton organization in cancer cells by inhibiting the mTOR complex 1 signaling pathway. *Cell Oncol (Dordr)*. 2020;43(5):793-805.
90. Zhou HY, Wong AS. Activation of p70S6K induces expression of matrix metalloproteinase 9 associated with hepatocyte growth factor-mediated invasion in human ovarian cancer cells. *Endocrinology*. 2006;147(5):2557-66.

91. Chan TO, Pascal JM, Armen RS, Rodeck U. Autoregulation of kinase dephosphorylation by ATP binding in AGC protein kinases. *Cell Cycle*. 2012;11(3):475-8.
92. Lazaro G, Kostaras E, Vivanco I. Inhibitors in AKTion: ATP-competitive vs allosteric. *Biochem Soc Trans*. 2020;48(3):933-43.
93. Rehan M, Bajouh OS. Virtual screening of naphthoquinone analogs for potent inhibitors against the cancer-signaling PI3K/AKT/mTOR pathway. *J Cell Biochem*. 2018.
94. Chorner PM, Moorehead RA. A-674563, a putative AKT1 inhibitor that also suppresses CDK2 activity, inhibits human NSCLC cell growth more effectively than the pan-AKT inhibitor, MK-2206. *PLoS One*. 2018;13(2):e0193344.
95. Vergara D, Simeone P, Franck J, Trerotola M, Giudetti A, Capobianco L, et al. Translating epithelial mesenchymal transition markers into the clinic: Novel insights from proteomics. *EuPA Open Proteom*. 2016;10:31-41.
96. Sun BO, Fang Y, Li Z, Chen Z, Xiang J. Role of cellular cytoskeleton in epithelial-mesenchymal transition process during cancer progression. *Biomed Rep*. 2015;3(5):603-10.
97. Katsuno Y, Lamouille S, Derynck R. TGF-beta signaling and epithelial-mesenchymal transition in cancer progression. *Curr Opin Oncol*. 2013;25(1):76-84.
98. Valcourt U KM, Niimi H, Heldin CH, Moustakas A. TGF- β and the Smad signaling pathway support transcriptomic reprogramming during epithelial-mesenchymal cell transition. *Molecular biology of the cell*. 2005;16(4):1987-2002.
99. Ábrigo J CF, Simon F, Riedel C, Cabrera D, Vilos C, Cabello-Verrugio C. TGF- β requires the activation of canonical and non-canonical signalling pathways to induce skeletal muscle atrophy. *Biological chemistry*. 2018;399(3):253-64.

REFERENCES



จุฬาลงกรณ์มหาวิทยาลัย
CHULALONGKORN UNIVERSITY



จุฬาลงกรณ์มหาวิทยาลัย
CHULALONGKORN UNIVERSITY

VITA

NAME Sutthaorn Pothongsrisit

DATE OF BIRTH 25 January 1995

PLACE OF BIRTH Bangkok

INSTITUTIONS ATTENDED Faculty of Pharmaceutical sciences, Chulalongkorn University

HOME ADDRESS 134/148 Bang Kruai-Sai Noi Rd.
Wat Chalor
Bang Kruai
Nonthaburi
11130